Geochemistry, Geophysics, Geosystems

RESEARCH ARTICLE
10.1029/2019GC008499

Key Points:
- Cenozoic volcanic rocks in SWNA separate into groups with high (~1), intermediate (0.2 to 0.6), and low (<0.2) Ta/Th values
- Volcanic rocks with intermediate Ta/Th values are common in SWNA but rare in oceanic settings
- The intermediate Ta/Th values reflect melting of metasomatized continental lithospheric mantle-bearing Ta- and Th-rich accessory minerals

Supporting Information:
- Supporting Information S1
- Figure S1
- Figure S2
- Data Set S1
- Movie S1

Correspondence to:
G. Lang Farmer,
farmer@colorado.edu

Citation:
Farmer, G. L., Fritz, D. E., & Glazner, A. F. (2020). Identifying Metasomatized continental lithospheric mantle involvement in Cenozoic Magmatism from Ta/Th values, southwestern North America. *Geochemistry, Geophysics, Geosystems*, *21*, e2019GC008499. https://doi.org/10.1029/2019GC008499

Received 10 JUN 2019
Accepted 22 MAR 2020
Accepted article online 24 MAR 2020

Identifying Metasomatized Continental Lithospheric Mantle Involvement in Cenozoic Magmatism From Ta/Th Values, Southwestern North America

G. Lang Farmer[1], Diane E. Fritz[2], and Allen F. Glazner[3]

[1]Department of Geological Sciences and CIRES, University of Colorado Boulder, Boulder, CO, USA, [2]Researcher Support Services, University of Colorado Denver, Denver, CO, USA, [3]Department of Geological Sciences, University of North Carolina, Chapel Hill, NC, USA

Abstract The accessory minerals rutile and apatite are rare or absent in the convecting upper mantle but occur in shallow, cooler, metasomatized continental lithospheric mantle (CLM) where they serve as carrier phases for the trace elements Ta (in rutile) and Th (in apatite). Because both minerals crystallize near-solidus and are eliminated early during partial mantle melting, the relative abundances of rutile and apatite should control the Ta and Th abundances of mantle melts and provide a means of identifying the involvement of rutile- and/or apatite-bearing metasomatized CLM in mafic continental magmatism. As a test, we investigated published Ta and Th abundances data from ~2,000 whole-rock samples of mafic to intermediate composition, Cenozoic volcanic rocks in southwestern North America. Roughly half of the samples have Ta/Th values similar to those of island arc volcanic rocks (<0.2) or ocean island and mid-ocean ridge basalts (>0.6). The remaining samples have intermediate and variable Ta/Th values between 0.2 and 0.6, independent of specific indices of crustal interaction (e.g., wt% P_2O_5/wt% K_2O). We interpret the intermediate Ta/Th rocks as the products of direct melting of, or of extensive melt-rock interaction with, rutile- and/or apatite-bearing CLM. Intermediate Ta/Th rocks also have uniformly high $^{87}Sr/^{86}Sr$ (0.706 to 0.708) compared to oceanic basalts that, unlike their Nd isotopic compositions, do not covary with lithospheric age. These observations are consistent with widespread metasomatism of the CLM by Sr-rich, Nd-poor, aqueous fluids generated by dehydration of oceanic lithosphere, and its overlying tectonic mélange during early Cenozoic subduction beneath southwestern North America.

Plain Language Summary Volcanism occurred throughout southwestern North America (SWNA) over the past 40 million years, but exactly what melted to produce the resulting volcanic rocks is unclear. We address this issue by investigating the relative amounts of the elements tantalum (Ta) and thorium (Th) in these volcanic rocks. In oceanic settings, volcanic rocks have well-defined Ta/Th values either from ~0.6 to ~1 for oceanic islands and ocean floor basalts or <0.2 for island-arc volcanoes. But in SWNA, approximately 40% of the ~2,000 volcanic rocks for which Ta and Th abundances are available have variable and intermediate Ta/Th values (0.2 to 0.6) that occur independently of chemical indicators used to identify interaction between continental crust and ascending magmas. We suggest that the intermediate Ta/Th values reflect melting of mantle directly beneath the continent that contains minerals that concentrate Ta and Th, such as rutile (a titanium oxide) and apatite (a calcium phosphate). Both minerals can precipitate from water-rich fluids that cool when infiltrating and altering the continental mantle but readily melt upon subsequent heating. We conclude that hydrated, rutile- and/or apatite-bearing continental mantle was widespread beneath SWNA and was an important contributor to the magmas from which the intermediate Ta/Th volcanic rocks were derived.

1. Introduction

Metasomatic alteration by aqueous fluids and/or melts likely provides a necessary preconditioning for subsequent partial melting of the continental lithospheric mantle (CLM), but identifying volcanic rocks derived from melting or extensive interaction with metasomatized CLM is challenging (Farmer, 2003, and references therein; Rooney et al., 2017). Nevertheless, identifying the presence of metasomatized mantle and the composition of metasomatizing fluids indirectly from volcanic rock compositions provides a unique method of investigating the evolution of the deep continental lithosphere. For example, there is increasing evidence from mantle-derived xenoliths that subduction-related aqueous fluid may be a common metasomatizing

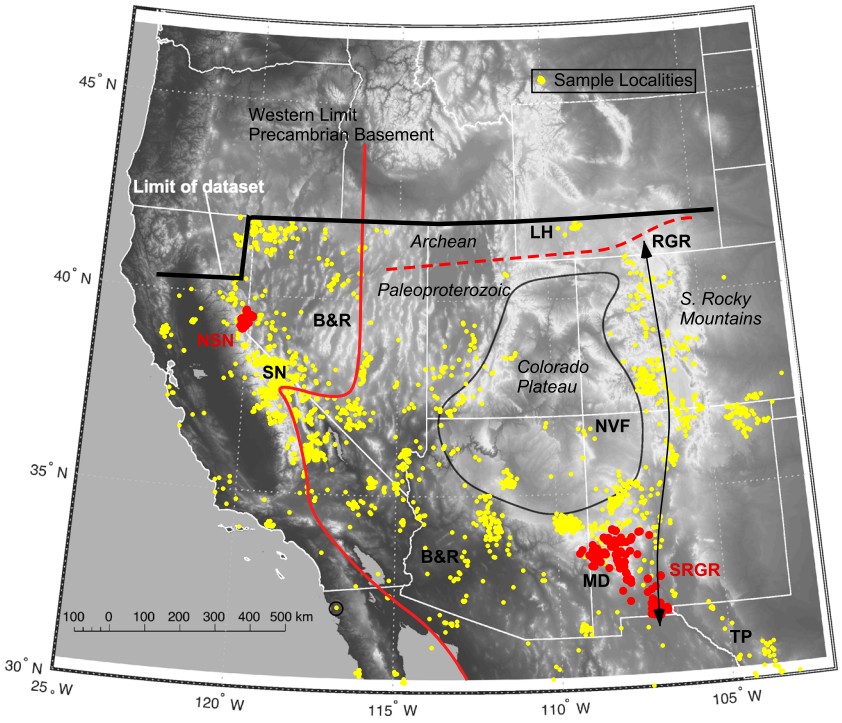

Figure 1. Map of SWNA with locations of volcanic rock samples included in data set. Samples from northern Sierra Nevada (NSN) and southern Rio Grande rift (SRGR) shown in red. Western limit of Precambrian basement from Kistler and Peterman (1973). LH = Leucite Hills, SN = Sierra Nevada, NVF = Navajo Volcanic Field, TP = Trans-Pecos, RGR = Rio Grande rift (arrowed line), B&R = Basin and Range province, MD= Mogollon-Datil Volcanic Field.

agent in the CLM (Fitzpayne et al., 2019; Schaffer et al., 2019). Minerals introduced to the CLM during such metasomatism can, in term, impart specific chemical signatures to continental volcanic rocks derived from such mantle. Relative depletions in K and Rb are commonly used to recognize the involvement of

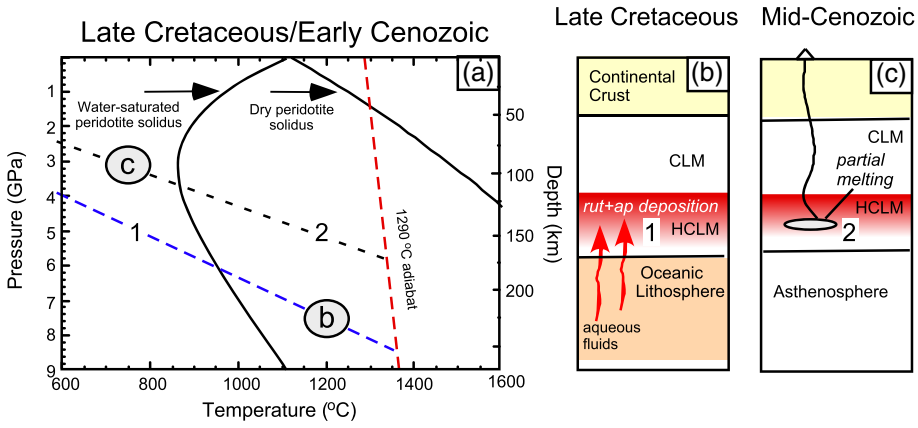

Figure 2. (a) Schematic steady-state conductive geotherm for continental lithospheric mantle during low-angle subduction of, and refrigeration by, oceanic lithosphere beneath SWNA in Late Cretaceous to early Cenozoic. Water-saturated and anhydrous peridotite solidii from Hirschmann (2000) and Mysen and Boettcher (1975). A 1290 °C adiabat for convecting mantle is shown for reference. Curves labeled "b" and "c" are steady-state geotherms for the scenarios shown in (b) and (c). (b) Schematic cross section through SWNA during Late Cretaceous/early Cenozoic Laramide Orogeny. Fluids generated in subducting oceanic lithosphere rise and cool in the CLM, resulting in hydration of lithosphere (HCLM) and precipitation of rutile ± apatite. (c) Same as (b), but for mid-Cenozoic, after the removal of oceanic lithosphere and upwelling of asthenosphere. Higher temperatures produced in HCLM after removal of oceanic lithosphere triggers partial melting. Positions marked "1" and "2" in (b) and (c), respectively, show temperatures at ~150 km depth in (a).

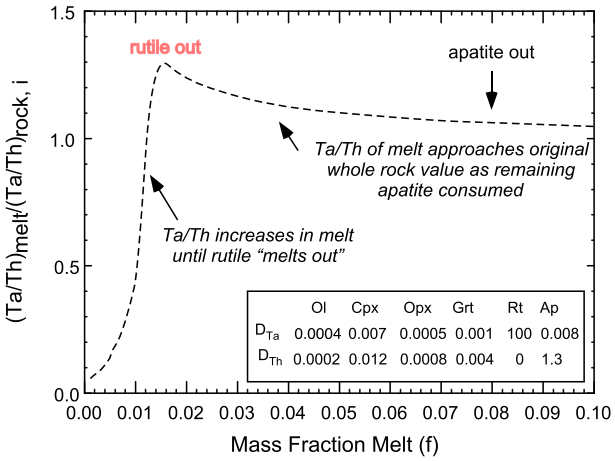

Figure 3. Melt Ta/Th (normalized to initial rock Ta/Th value) versus mass fraction of melt (f) for non-modal, batch melting of a rutile ± apatite-bearing metasomatized garnet peridotite. Initial relative masses of cpx, opx, ol, and gar set at 4:40:52:4 and the non-modal melting reaction of garnet peridotite used from Walter (1998) (7 olivine + 68 cpx + 25 garnet = 84 melt + 16 opx). Initial masses of apatite and rutile set at 4 and 1.2 mg/g_{rock}, respectively. Initial Th and Ta concentrations for apatite and rutile set at 12.3 and 4,000 ppm, in ranges expected for rutile and apatite in the upper mantle (Klemme et al., 2005; O'Reilly & Griffin, 2000). Mineral-melt partition coefficients (D) for Ta and Th in major and accessory mineral phases listed on diagram from GERM partition coefficient (Kd) database. Solubilities of rutile and apatite in basaltic melt set at 10% and 5%, respectively (Ryerson & Watson, 1987; Watson, 1980).

phlogopite-bearing, modally metasomatized CLM in the generation of potassic continental volcanic rocks (Furman & Graham, 1999; Johnson et al., 2005; Pfänder et al., 2018).

In this study, we investigate whether the mass ratio of tantalum to thorium (Ta/Th) can be used in a similar fashion to identify continental volcanic rocks derived from fluid metasomatized CLM. Both Ta and Th are trace elements, but Ta is a high field strength element (HFSE) whereas Th is an actinide with significantly different geochemical behavior (White, 2015). One key distinction is that in the uppermost mantle these elements partition preferentially into different accessory mineral phases: Ta into oxides, most commonly rutile (TiO_2), and Th into phosphates such as apatite, $Ca_5(PO_4)_3(OH, F, Cl)$. When present in the mantle, rutile serves as the primary host (e.g., carrier phase) for Ta, and apatite is the host for Th and for P (O'Hara et al., 2001a, 2001b; Smith, 1981). Critical for our purposes is the fact that precipitation of rutile and apatite can accompany aqueous metasomatism of shallow, lithospheric mantle (O'Reilly & Griffin, 2013). Because both minerals only start to crystallize near the solidus and are fully consumed after only a few percent partial mantle melting (Ryerson & Watson, 1987; Watson, 1980), melts of rutile- and apatite-bearing lithospheric mantle should have variable Ta/Th values largely controlled by the original abundances of these metasomatic accessory phases in the altered mantle.

In this study we use published Ta/Th values from Cenozoic volcanic rocks in SWNA to demonstrate that mafic to intermediate volcanic rocks ultimately derived from rutile ± apatite-bearing mantle sources are abundant in this region. This conclusion implies that metasomatized continental lithospheric mantle was also widespread. The metasomatism may have been caused by aqueous fluids generated from oceanic lithosphere that was subducted at shallow angles beneath the continent during the Late Cretaceous/early Cenozoic Laramide Orogeny.

2. Background Information

Throughout much of the Mesozoic, westernmost SWNA was a convergent plate boundary, and magmatism was largely restricted to a continental margin arc responsible for the formation of the Sierra Nevada and other continental margin batholiths (Figure 1) (Dickinson, 2004). Magmatism ceased along the continental arc in the Late Cretaceous, most likely in response to an episode of low-angle subduction of oceanic lithosphere (the Farallon Plate) related to the Laramide Orogeny, which produced basement-cored uplifts some 1,000 km inboard of the continental margin (English & Johnston, 2004; Saleeby, 2003). Magmatism was sparse in much of the southwestern United States during the Laramide Orogeny (Jones et al., 2011), but arc volcanism did migrate from west to east across northern Mexico during this time (González-León et al., 2011). In the Oligocene, voluminous intermediate to silicic composition magmatism affected much of SWNA, including the southern Rocky Mountain region (Figure 1) (Lipman et al., 1972). After this ignimbrite flare-up, lithospheric extension and associated basaltic volcanism occurred diachronously across SWNA during the formation of the Basin and Range province (Figure 1) (Coney & Reynolds, 1977; Glazner & Ussler, 1989; Lipman et al., 1971; Snyder et al., 1976). In the late Cenozoic, oceanic ridge and trench intersection at the western margin of the continent resulted in the formation of the San Andreas transform fault system that currently separates the Pacific and North American plates and triggered the development of a progressively enlarging slabless window beneath the southwestern United States (Atwater & Stock, 1998).

Our interest in this paper is in assessing whether the Cenozoic magmatic evolution of SWNA was influenced by widespread hydration of the continental lithospheric mantle (CLM) during the Laramide Orogeny (Humphreys et al., 2003). For example, one possible trigger mechanism for the ignimbrite flare-up was rollback of the Farallon Plate that exposed deep portions of the CLM to upwelling asthenosphere, inducing melting in CLM that had been refrigerated and hydrated as a result of underthrusting of oceanic

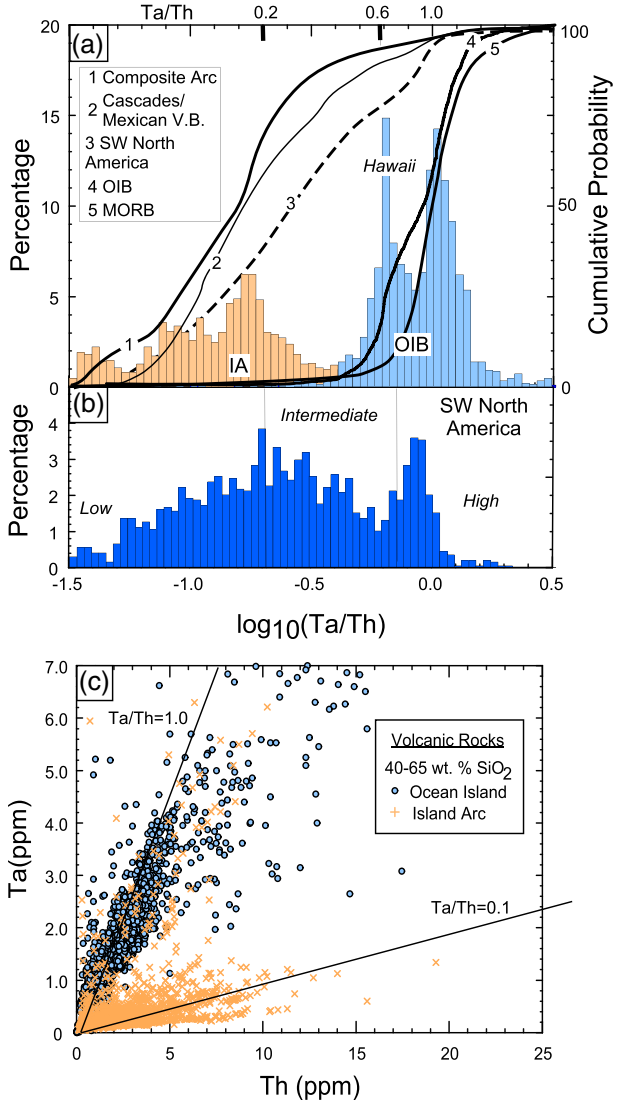

Figure 4. (a) Relative histograms (left hand axis) and cumulative probability plots (right hand axis) of $\log_{10}$(Ta/Th) values for selected volcanic rock suites. Ocean island basalt (OIB) data are from precompiled data sets available from geochemistry of rocks of the oceans and continents (GEOROC) (http://georoc.mpch-mainz.gwdg.de/georoc/) and include data from Hawaii, Kerguelen, Mascarene, Samoa, and St. Helena (n_{total} = 1,996). Cumulative probability curve for mid-ocean ridge basalts (MORB) constructed from Mid-Atlantic Ridge basalt data delivered by PetDB (n = 775; http://www.earthchem.org/petdb). Composite island arc (IA) volcanic rock data are for 40 to 65 wt% SiO_2 calc-alkalic rocks in various Pacific Ocean island arcs (Aleutian, Izu-Bonin, Kurile, and Mariana Islands; n_{total} = 2,556) and were extracted from precompiled data sets available from GEOROC. Combined cumulative probability curve for the Cascade (northwest United States) and Mexican volcanic belt (southern Mexico) continental margin arcs also constructed from data for 40 to 65 wt% SiO_2 volcanic rocks available in precompiled data set from GEOROC (Cascade volcanic arc) and from NAVDAT (http://www.navdat.org) (n_{total} = 935). (b) Histogram of $\log_{10}$(Ta/Th) for our data set from SWNA (n = 1,975). Cumulative probability curve for this data set is shown as curve "3" in (a). (c) Ta (ppm) versus Th (ppm) for oceanic and composite island arc volcanic rocks compiled in (a).

lithosphere beneath the continent during the earlier Laramide Orogeny (Figures 2b and 2c) (Dumitru et al., 1991; Farmer et al., 2008).

Direct evidence of metasomatism in SWNA comes in the form of mantle xenoliths entrained in late Cenozoic volcanic rocks, many of which show the effects of interaction with $H_2O \pm CO_2 \pm$ Cl fluids (Lee, 2005) similar to that found in mantle xenoliths from "off-craton" localities worldwide (O'Reilly & Griffin, 2013). In the SWNA xenoliths, metasomatically introduced minerals occur in veins, alteration haloes, and/or as precipitates in fluid inclusions and are dominated by amphibole ± phlogopite with lesser amounts of carbonate ± chlorapatite ± spinel ± rutile (Nielson et al., 1993; Wang et al., 1999). Metasomatized examples of both spinel and garnet peridotite xenoliths are known (Lee, 2005; Li et al., 2008; Smith, 2010). Isotopic age determinations from metasomatic accessory minerals in mantle and lower crustal xenoliths from the Oligocene Navajo Volcanic Field on the Colorado Plateau (Figure 1) suggest that metasomatism beneath these locations occurred during the Laramide Orogeny in the Late Cretaceous to Paleogene (Butcher et al., 2017; Smith & Griffin, 2005).

Of particular import are mantle-derived garnet xenocrysts found at the Navajo Volcanic Field which contain rutile- and chlorapatite-bearing aqueous fluid inclusions (Wang et al., 1999). The possibility that apatite or rutile, or both, are present in the metasomatized mantle is the basis for our approach to identifying the involvement of such mantle in the generation of Cenozoic volcanic rocks in SWNA. In general, rutile is rare, and apatite unstable in the sublithospheric mantle (hereafter referred to as asthenosphere) (Ionov, 2010; Konzett & Frost, 2009). The occurrence of both phases in Earth's mantle is instead limited to metasomatized lithosphere. For metasomatism by aqueous fluids, this likely relates to changes in rutile and apatite solubilities in fluids ascending through the lithospheric mantle. The solubilities of both phases increase with increasing fluid NaCl (or Na silicate) contents and with increasing temperature and pressure (Antignano & Manning, 2008a, 2008b; Mair et al., 2017). Although there are no experimental data available for pressures corresponding to the base of the continental mantle lithosphere, at crustal pressures the solubilities of these phases decrease by a factor of four or more as fluid temperatures decrease from 1,000 to 800 °C. Aqueous fluids containing Ti and P and ascending and cooling through this temperature range in the lithospheric mantle could therefore precipitate rutile and apatite (Figure 2b) (Ayers & Watson, 1991; Tanis et al., 2016). An indication of the presence of rutile and/or apatite in the source of a continental, mantle-derived volcanic rock could thus represent evidence of the involvement of metasomatized CLM in the generation of its parental melt.

Apatite and rutile contain over 90% of Th and Ta, respectively, in metasomatized peridotites (Bodinier et al., 1996; O'Reilly & Griffin, 2000). In such rocks, whole-rock Ta/Th values depend on the mass ratio of apatite to rutile which varies as a function of the conditions and intensity of mantle metasomatism. We propose that this variability in Ta/Th is inherited by partial melts of metasomatized mantle and provides a fingerprint of its involvement in the generation of continental volcanic rocks.

We cannot fully define the Ta/Th values expected in melts derived from apatite- and rutile-bearing mantle given the number of variables involved, including the initial masses of rutile and apatite in the metasomatized mantle and their Th and Ta contents, the relative solubilities of the two

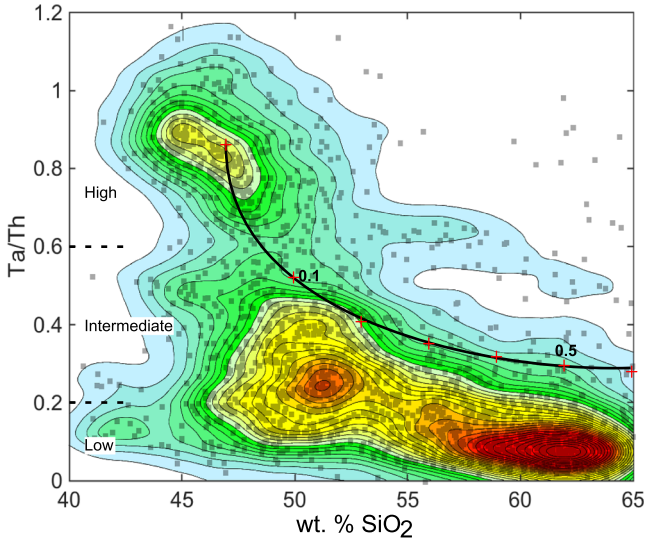

Figure 5. Ta/Th versus wt% SiO_2 for 0–40 Ma volcanic rocks from SWNA plotted as smoothed 2-D histogram. Boundary values for three groups of Ta/Th values (defined in text) shown as dashed lines. Line show products of simple mixing of a high Ta/Th mafic melt with a silicic melt produced by anatexis of Precambrian mafic continental crust in southern Rocky Mountains, labeled by fraction of latter in mixture (see text for description).

phases in the melt, the relevant mineral-melt partition coefficients for Ta in rutile and Th in apatite, and the extent of partial melting. But some basic constraints are possible based on the fact that rutile is up to three times more soluble than apatite in basaltic composition melts (~15% TiO_2 vs. 4–6% P_2O_5 at 2.5 Ga and 1350 °C) (Gaetani et al., 2008; Ryerson & Watson, 1987; Watson, 1980). When combined with the fact that apatite can constitute as much as 1 vol% of metasomes in peridotite (O'Reilly & Griffin, 2000), but rutile is typically present in exceptionally low abundances (<0.01%) (Kalfoun et al., 2002), the experimental results suggest that melting of apatite- and rutile-bearing peridotite will eliminate rutile, but not apatite, from the residual solid even at low extents of partial melting (<~1%) (Figure 3). The Ta/Th values of batch melts produced under these conditions show a typical pattern as melting proceeds, with the values reaching a maximum where rutile is exhausted from the solid residue and then gradually approaching the original whole-rock value as apatite is progressively eliminated from the solid with further melting (Figure 3). Because basalts typically represent >5% melting of peridotite (Kushiro, 2001) these considerations suggest that a basalt derived from apatite- and rutile-bearing metasomatized mantle will have a Ta/Th value similar to that of its source rock, with the source rock Ta/Th value being controlled largely by the relative masses of the two minerals in the original solid.

We emphasize that melts of apatite ± rutile-bearing mantle will inherit whole-rock Ta/Th values once the carrier phases are eliminated from the solid residue even if a mineral remains that can accommodate some of the carrier element (e.g., Ta in amphibole; Adam et al., 1993). Such residual phases can only accommodate a small fraction of the original whole-rock complement of either Ta or Th provided that the mineral/melt partition coefficient for this phase is less than unity (Ionov & Hofmann, 1995).

In the absence of rutile or apatite both Ta and Th are strongly incompatible (Hauri et al., 1994; McDonough et al., 1992). Incompatible behavior for these elements can account for the nearly constant Ta/Th values of mid-ocean ridge basalts (MORB) and ocean island basalts (OIB) (~0.6 to 1.1; Figure 4a) (Hanson, 1989; McDonough et al., 1992). In contrast, the relative abundances of Ta and Th in island arc volcanic rocks are influenced not just by their partitioning during partial mantle melting but also the abundance of both elements in fluids and melts generated from downgoing oceanic lithosphere (Bailey & Ragnarsdottir, 1994; Plank & Langmuir, 1993). In general, both Ta and Th are relatively immobile in aqueous fluids, particularly compared to large ion lithophile elements, but can be mobilized in melts of oceanic crust, subducted sediments, or subduction mélanges (Nielsen & Marschall, 2017). Nevertheless, the Ta/Th values of island arc volcanic rocks vary over only a narrow range, albeit at lower Ta/Th (<0.2) than either MORB or OIB (Figure 4a). The low Ta/Th, low Ta abundances (Figures 4a and 4c), and overall low ratios of high field strength elements (HFSE) to large ion lithophile elements (LILE) in these rocks are commonly, but not universally (Baier et al., 2008), attributed to the role of residual rutile in subducting oceanic lithosphere (Kelemen et al., 2014).

Regardless of the origin of the low HFSE/LILE in arc volcanic rocks, their low Ta/Th values provide a clear fingerprint of volcanic rocks generated by active arc magmatism (Figures 4a and 4c). Similarly, the uniformly high Ta/Th values for OIB and MORB provide a convenient method of identifying melts derived from the asthenospheric mantle (Figures 4a and 4c). But variable Ta/Th values in a group of continental, mantle-derived, volcanic rocks may provide a signature of the involvement of variably metasomatized, rutile- and/or apatite-bearing CLM in their generation.

We emphasize that while Ta/Th ratios may not be uniquely suited to our purposes, element pairs with similar properties are rare. For example, Rb and La are both strongly incompatible elements during mantle melting but can be concentrated in the lithospheric mantle in the accessory minerals phlogopite and apatite (Chazot et al., 1996; Schmidt et al., 1999). The Rb/La values of OIB/MORB are relatively constant, but

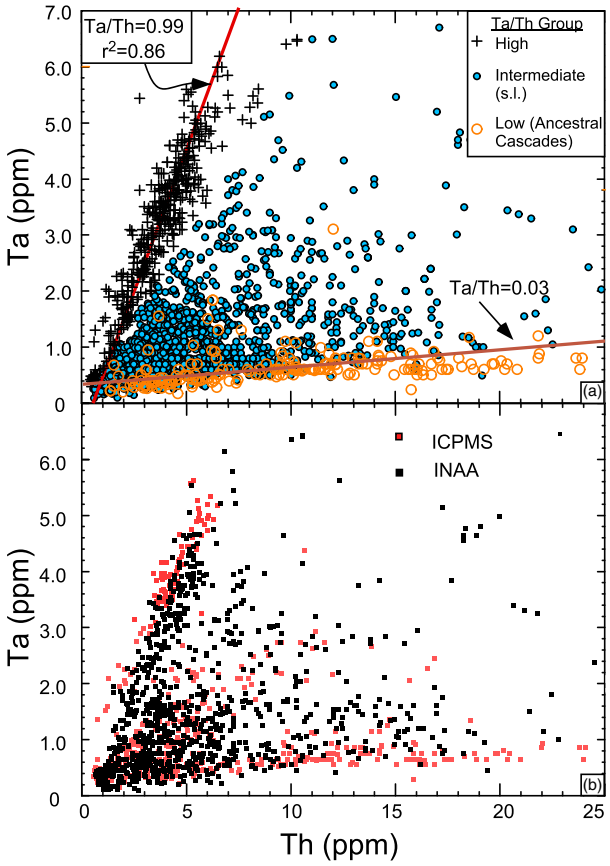

Figure 6. (a) Ta (ppm) versus Th (ppm) for our data compilation. Line drawn at Ta/Th = 0.99 fit through data from high Ta/Th group. Low Ta/Th group includes only volcanic rocks from eastern California and western Nevada. (b) Ta (ppm) versus Th (ppm) for samples for which both Ta and Th abundances were determined either by ICPMS (red symbols) or by instrumental neutron activation analyses (INAA; black symbols).

Rb/La values for arc volcanic rocks are variable and overlap the range of values found for OIB/MORB, likely due to the mobility of Rb in fluids generated during subduction that interact with the mantle sources of arc volcanic (Supporting Information Figure S1) (Zheng, 2019). In contrast, the Ta/Th values of MORB/OIB and arc volcanic rocks are cleanly separable, largely because of the uniformly low Ta abundances of arc rocks.

SWNA is an ideal location to test the utility of Ta/Th values in identifying the role of metasomatized CLM in continental magmatism because of the possibility that widespread aqueous metasomatism of lithospheric mantle occurred during the Laramide Orogeny (Humphreys et al., 2003). Furthermore, Cenozoic volcanic rocks are widespread in this area, and the Ta/Th values of these rocks could document the occurrence and geographic extent of any metasomatized CLM, an assessment not possible on the basis of the relatively few occurrences of mantle xenoliths (Wilshire et al., 1988).

3. Data

For this study we compiled chemical data from >5,000, Oligocene and younger mafic to intermediate composition rocks (40 to 65 wt% SiO_2) available from NAVDAT (Walker et al., 2006; available at earthchemportal.org) and supplemented by a number of other literature sources. A list of these additional sources and the entire data set are available in Supporting Information S1 and Data Set S1, respectively.

Dacites and rhyolites were excluded from our data compilation because higher silica igneous rocks in western North America can be the products of crustal melting and, as a result, their Ta/Th values have no bearing on mantle values (Christiansen & McCurry, 2008). In addition, accessory phases can crystallize from silicic melts and can significantly modify Ta/Th values during crystal fractionation (Padilla & Gualda, 2016).

For the selected analyses, major element oxide abundances were corrected to 100% anhydrous but were otherwise unmodified. Mis-entered data delivered by NAVDAT were corrected using the original data source. Most of the samples are from the southern Rocky Mountains and the Basin and Range province between 22°N and 42°N latitudes, areas underlain principally by Proterozoic continental lithosphere or younger accreted terranes (Figure 1) (Whitmeyer & Karlstrom, 2007).

The data set includes 1,975 samples for which Ta and Th concentration data are available. We chose to assess Ta abundances rather than Nb, which is geochemically almost identical to Ta, because of the high detection limits (~2 ppm) for the X-ray fluorescence-based determinations of Nb typically employed pre-1990s. In contrast, both Ta and Th determinations in older data sets are generally instrumental neutron activation analyses (INAA) which has low detection limits of ~ 0.01 ppm for both elements (Potts, 1997). Post-1990s concentrations determinations for Ta and Th are typically by inductively coupled plasma mass spectrometry (ICP-MS). External reproducibilities for Th analyses are similar (~3%) for INAA and ICP-MS, but better by a factor of two for Ta concentrations by the latter technique. However, considering the wide range of Ta abundances observed in our data set (~0.1 to ~10 ppm), the differences in external reproducibilities for Ta determinations by INAA and ICP-MS do not affect our ability to discriminate between volcanic rocks on the basis of Ta/Th values.

We chose to assess Th abundances, and not U, because Th (along with Ta) is considered immobile during surficial weathering of mafic to intermediate compositions volcanic rocks whereas U is mobile under oxidizing conditions (Aiuppa et al., 2000; Kurtz et al., 2000). As a result, rock Ta/Th values, but not elemental ratios involving U abundances, should be unmodified by surficial weathering.

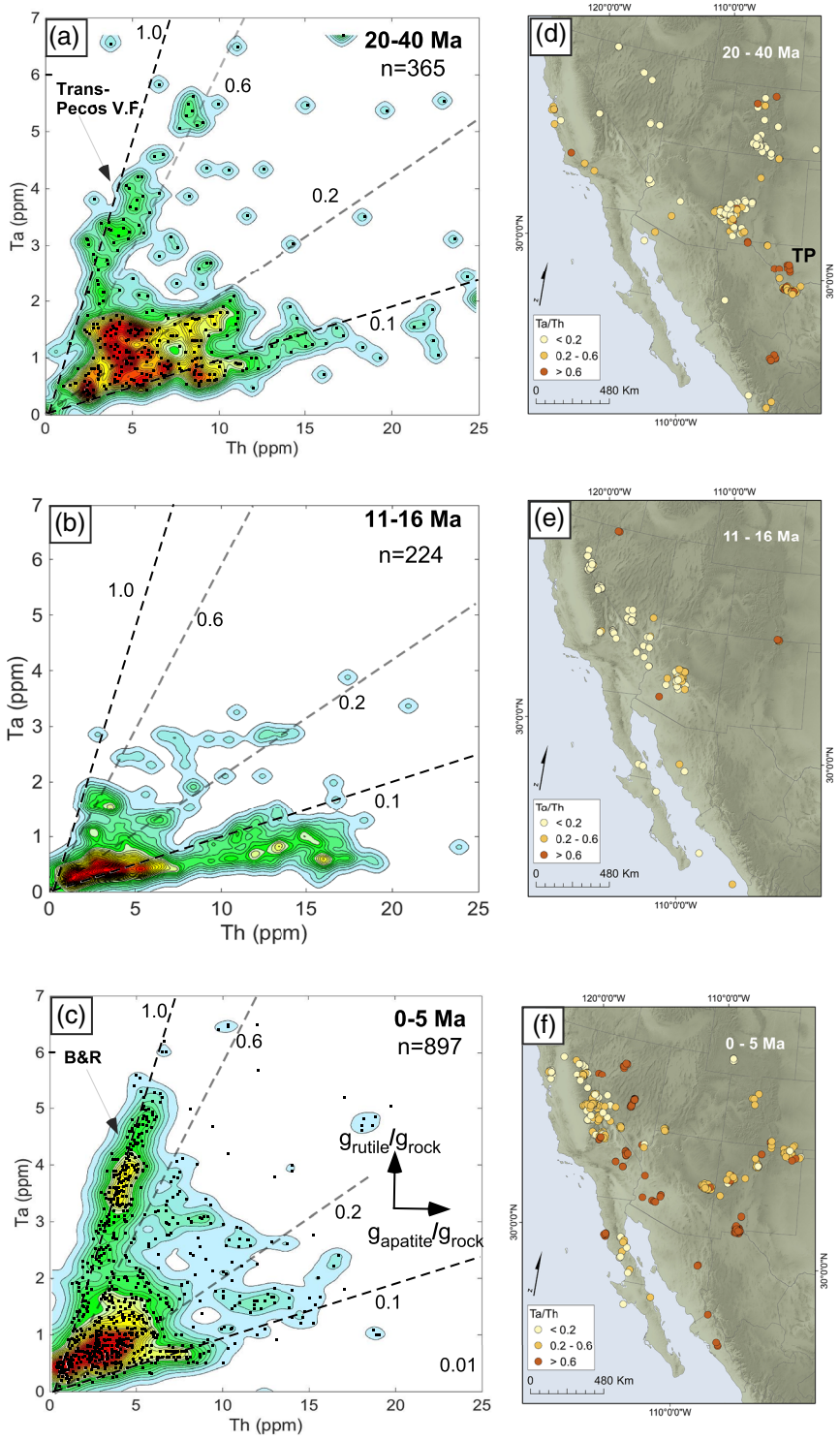

Figure 7. (ac) Ta (ppm) versus Th (ppm) for volcanic rocks from three time slices: (a) 20–40, (b) 11–16, and (c) 0–5 Ma. Individual data points are shown superimposed on smoothed 2-D histograms (n = number of analyses plotted). Red-shaded areas encompass ~50% of analyses in a given time slice. Arrows show effect on melt compositions of increasing abundance ($grams_{mineral}/gram_{whole\ rock}$) of either rutile or apatite in a metasomatized mantle source. Dashed lines are constant Ta/Th for labeled values. (df) Map locations for volcanic rock samples in three Ta/Th groups for each time slice. TP = Trans-Pecos Volcanic Field. Movie showing continuous variations in Ta versus Th from 40 to 0 Ma is available in Movie S1.

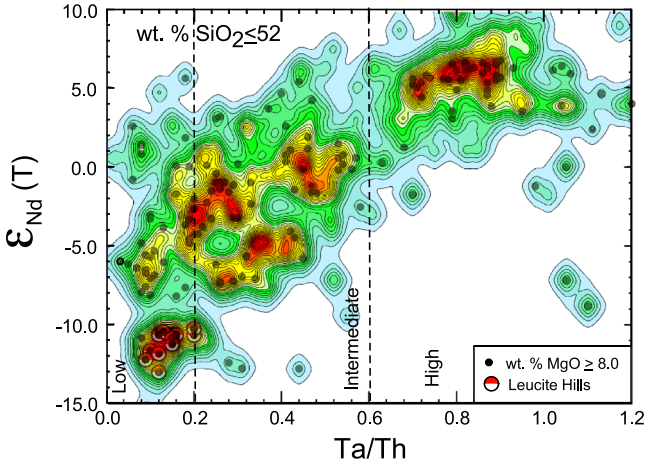

Figure 8. ε_{Nd} (T) versus Ta/Th for Cenozoic basalts (<52 wt% SiO_2) in SWNA, plotted as smoothed 2-D histogram. Samples with ≥8 wt% MgO shown as filled circles. Leucite Hills leucitites from the southern margin of Archean Wyoming Craton also plotted separately to illustrate their lower ε_{Nd} (T) values compared to other volcanic rocks.

Smoothed 2-D histograms provide a simple means of visualizing data density in large data sets (Eilers & Goeman, 2004), and we use this approach in many of our data plots. Data density reflects the frequency of specific chemical parameters, such as Ta/Th values, in the data set and should not be construed as a proxy for the original eruptive volumes of volcanic material of any given composition. Our illustrations simply reveal the Ta/Th characteristics (ranges and population densities) of the compiled data.

4. Results

Most of the volcanic rock Ta/Th values in our compilation range from ~0.01 and ~1.2, with clusters of higher data density at high (0.6 to 1.1), intermediate (0.6 to 0.2), and low (<0.2) values (Figure 5). Rocks with high Ta/Th values (0.6 to 1.1) comprise ~20% of our data set and cluster at low SiO_2 (<50 wt%). Rocks with low Ta/Th values (<0.2) represent ~40% of our compilation and have a wide range of wt% SiO_2, but with the highest data density occurring at >55 wt% SiO_2. The Ta/Th values do not vary consistently with wt% SiO_2 in this group, although higher silica rocks (>55 wt%) have slightly lower values (<0.1). The remaining samples have intermediate Ta/Th values between 0.2 and 0.6. The majority of the samples in this group have wt% SiO_2 from 46 to 55 and Ta/Th values that scatter between 0.2 and 0.6, independently of silica contents.

The range of Ta and Th concentrations of the three volcanic rocks groups are also distinct (Figure 6a). The Ta and Th contents of the high Ta/Th group are correlated with one another, and Ta concentrations are high (up to 7 ppm). The low Ta/Th rocks have uniformly low Ta contents (<1 ppm). The intermediate Ta/Th group rocks have variable Ta and Th contents that range to values as high as 7 and 25 ppm, respectively.

The variations in the volcanic rock Ta/Th values in our data set are unlikely to be the result of analytical uncertainties in the Ta and/or Th abundances even though we included lower quality XRF and INAA abundance determinations. Regardless of the analytical technique used, similar groupings in volcanic rocks Ta/Th values are evident (Figure 6b). In addition, samples for which both Nb and Ta abundances are available, 90% have Nb/Ta values characteristic of terrestrial rocks (~15–20; not shown) (Tang et al., 2019), which argues against the possibility that systematic errors in legacy Ta concentration data could account for the observed variability in Ta/Th values. Another possibility is that variable Ta/Th

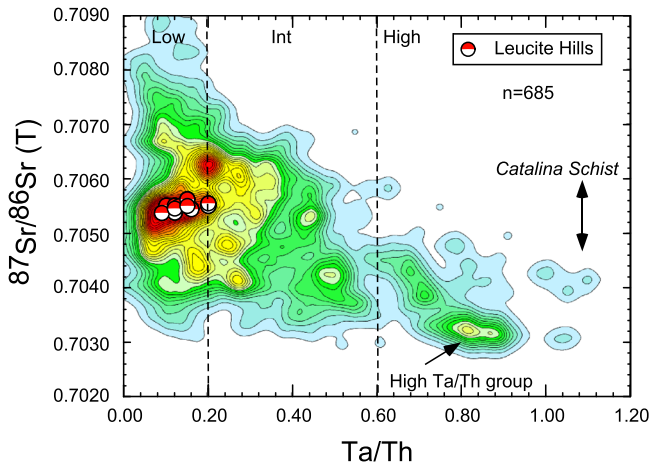

Figure 9. Volcanic rock initial $^{87}Sr/^{86}Sr$ (T) versus Ta/Th as 2-D histogram. Range of initial $^{87}Sr/^{86}Sr$ for fluid-mobile Sr in Catalina Schist in Late Cretaceous from King et al. (2006). Data for leucitites in Leucite Hills in southern Wyoming plotted separately. Dashed lines are boundaries between three Ta/Th groups as in Figure 5. All volcanic rock $^{87}Sr/^{86}Sr$ (T) overlap values for fluid-mobile Sr in the Catalina Schist, with exception of high Ta/Th group.

values are the result of Ta contamination of rock powders produced in tungsten carbide grinding vessels (Hickson & Juras, 1986). Information on grinding vessels is not compiled in on-line databases, but the distinction between various Ta/Th groups remains apparent even in rock powders known to have been ground in ceramic vessels (Farmer et al., 2013).

5. Discussion

Consideration of virtually all the trace element data available for ≤40 Ma basalts and andesites in SWNA reveals that these rocks cluster into groups with high, intermediate, and low Ta/Th values. The high Ta/Th group is correlative with OIB and MORB. In SWNA these rocks are mainly sodic basalts (<50 wt% SiO_2) that erupted throughout the Basin and Range province after the inception of extensional tectonism in SWNA 30 million years ago (Figures 7a, 7c, 7d, and 7f) (Leeman & Rogers, 1970). The basalts have high HFSE/LILE values, high wt% TiO_2 (>2), high ε_{Nd} (T) values (>+3; Figure 8), and low initial $^{87}Sr/^{86}Sr$ values (<0.7040; Figure 9) that all overlap with values for ocean island basalts (Farmer et al., 1995). These characteristics, along with their high Ta/Th values, are consistent with an origin via decompression melting of upwelling, rutile- and apatite-free, asthenospheric mantle triggered by lithospheric thinning (DePaolo & Daley, 2000; Fitton et al., 1991; James & Henry, 1991; Perry et al., 1987).

Similarly, some of the low Ta/Th group volcanic rocks are equivalent to island and continental margin arc volcanic rocks. The most prominent examples are 11 to 16 Ma basaltic andesites and andesites that erupted in northeastern California and western Nevada (Figures 7b and 7e) (Cousens et al., 2008; John et al., 2012). Previous workers have interpreted the overall trace element characteristics of these rocks (e.g., low HFSE/LILE) as evidence they are related to active arc magmatism of the "Ancestral Cascades" and are the products of melting of the slab-fluid metasomatized mantle wedge above actively subducting oceanic lithosphere beneath western North America (John et al., 2012). This conclusion is consistent with the uniformly low Ta abundances and uniformly low Ta/Th values (~0.03) characteristic of these volcanic rocks (Figure 6), which are similar to the compositions of individual Pacific island arc stratovolcanoes and of continental margin arc rocks of the modern Cascades and the Mexican Volcanic Belt in SWNA (Figure 4a).

In contrast, intermediate Ta/Th group volcanic rocks are uncommon in oceanic settings (Figure 4a) but comprise at least 40% of the rocks in our data set (Figure 4b). These rocks occur throughout SW North America, including the southern Rocky Mountains and the southern margins of the Colorado Plateau (Figure 7). Our principal interest is whether the Ta/Th values of these rocks represent evidence of the derivation of their parental magmas from rutile + apatite-bearing metasomatized CLM. However, it must first be established that their Ta/Th values were inherited from their mantle source regions and do not reflect changes in magma Ta/Th values during open or closed-system magmatic differentiation during ascent to the surface.

We address the latter issues from both a regional perspective, using the data set in toto, and from a local one using two data subsets comprising volcanic rocks from the northern Sierra Nevada and the southern Rio Grande rift and vicinity (Figure 1). These two locations were chosen for detailed study because they have different lithospheric ages, geologic histories, and different time intervals of active volcanism. The northern Sierra Nevada represents a portion of the Mesozoic Sierra Nevada batholith that formed at the continental margin and was built on Paleozoic crust accreted to the margin of the North American continent during the late Paleozoic to Triassic (Figure 1) (Dickinson, 2004). Cenozoic volcanism in this region commenced in the Miocene with basaltic andesites to dacites interpreted as products of continental arc magmatism related to the Ancestral Cascades (Figure 10d) (Cousens et al., 2008). Pliocene and younger volcanic rocks are principally trachybasaltic andesites to trachyandesites (Figure 10d) that represent post-subduction volcanism that occurred after the passage of the Mendocino Fracture Zone and the possible opening of a slabless window beneath this portion of northern California (Cousens et al., 2008).

The southern Rio Grande rift developed within Paleoproterozoic continental lithosphere (Figure 1). In this region, post-40 Ma volcanism resulted in the voluminous intermediate to silicic composition volcanic rocks of the Mogollon-Datil volcanic field, which is a part of the silicic ignimbrite flare-up that affected the southern Rocky Mountain region in the Oligocene (Figure 10a) (Elston et al., 1973). After 20 Ma, and in concert with the onset of lithospheric extension in this region, volcanism became dominantly basaltic both in the Rio Grande rift and along the SE margin of the adjacent Colorado Plateau (Figure 10a) (Baldridge et al., 1991).

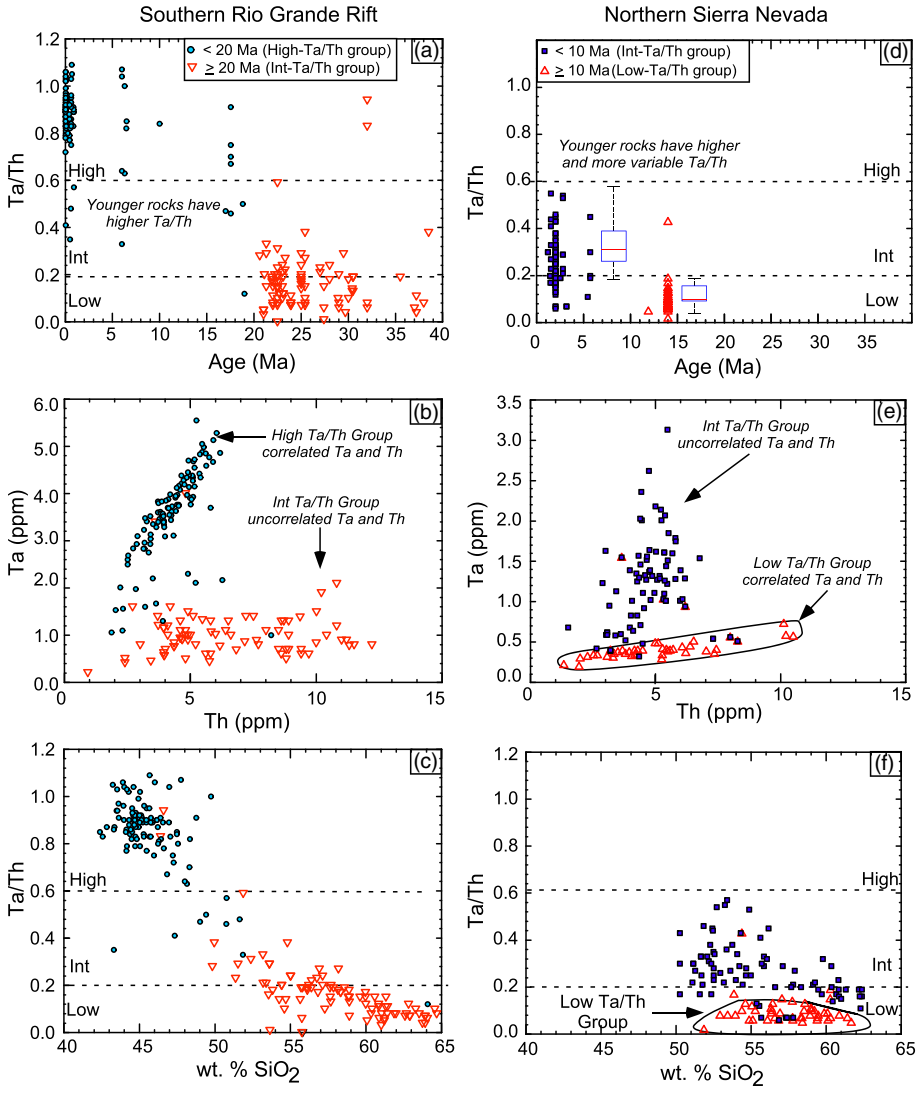

Figure 10. Ta/Th versus age (a, d), Ta versus Th contents (b, e), and Ta/Th versus wt% SiO_2 (c, f) for volcanic rocks in southern Rio Grande rift and northern Sierra Nevada. Box plots in (d) show mean and scatter of Ta/Th values for mafic (≤52 wt% SiO_2) intermediate Ta/Th group rocks (left) and older, low Ta/Th rocks (right) in the northern Sierra Nevada.

Older, Late Cretaceous, intermediate composition volcanism also occurred in this region and is interpreted as arc magmatism that occurred some 1,000 km inboard of the continental margin, possibly as a consequence of low-angle subduction of oceanic lithosphere during the Laramide Orogeny (Amato et al., 2017; Lawton & McMillan, 1999).

5.1. Role of Crustal Interaction in Intermediate Ta/Th Group Volcanic Rocks

One explanation for the intermediate Ta/Th values is that they are the result of interaction between asthenosphere-derived, mafic magmas and preexisting continental crust. This possibility has been investigated in detail as an explanation for the widespread occurrence of Cenozoic basalts with "crustal" Nd isotopic compositions in SWNA, ε_{Nd} (T) <+3, a category that includes all of the intermediate Ta/Th group basalts (Figure 8) (Beard & Johnson, 1997; Brandon et al., 1993; Glazner & Farmer, 1992; Menzies et al., 1985). However, most low ε_{Nd} (T) basalts lack a consistent correlation between their Nd isotopic compositions and wt% P_2O_5/wt% K_2O (P/K), both of which are expected to decrease with increasing

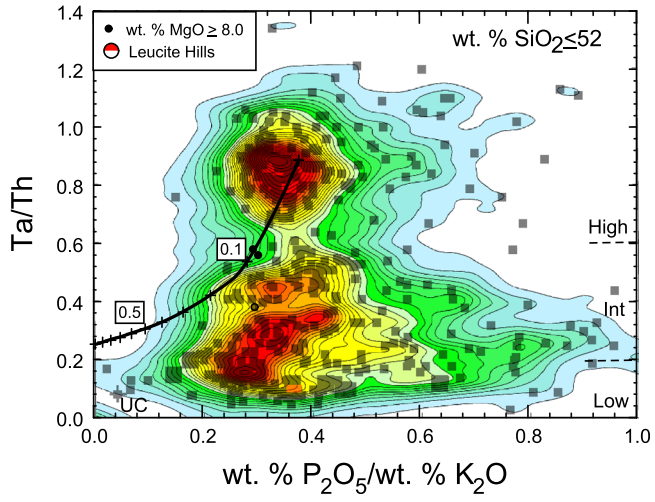

Figure 11. Ta/Th versus wt% P_2O_5/wt% K_2O for mafic rocks with ≤52 wt% SiO_2 in our data set plotted as 2-D histogram. Filled circles are samples with ≥8 wt% MgO. UC = average upper crust (Rudnick & Gao, 2003). Line shows products of simple mixing of a high Ta/Th mafic melt with a silicic melt produced by anatexis of Precambrian mafic continental crust in southern Rocky Mountains, labeled by fraction of latter in mixture (see text for description).

amounts of crustal assimilation because of the lower P/K and ε_{Nd} (T) values of average continental crust relative to asthenosphere-derived mafic magmas (Carlson & Nowell, 2001; Farmer et al., 2002).

A similar argument can be applied to variations in basalt Ta/Th values. Because average intermediate to upper continental crustal has low Ta/Th values (Ta/Th ~0.125) (Rudnick & Gao, 2003), interaction between high Ta/Th, asthenosphere-derived mafic melts, and intermediate to silicic composition crust should also produce decreasing Ta/Th with decreasing P/K, irrespective of the mode of crustal interaction (Figure 11). However, Ta/Th and P/K values are uncorrelated in the basalts in our data set, even for the most primitive rocks (>8 wt% MgO) (Figure 11). Instead, each of the Ta/Th groups are represented among the most mafic volcanic rocks and have overlapping P/K values (~0.2 to ~0.5). Intermediate Ta/Th group basalts do range to higher P/K values than those of the high Ta/Th, asthenosphere-derived rocks, but this is the opposite of what would be expected if the intermediate Ta/Th group rocks were the product of crustal interaction by high Ta/Th mafic magmas (Figure 11).

Evidence for crustal interaction between mafic magmas and continental crust occurs in andesitic Cenozoic volcanic rocks in western North America (Christiansen & McCurry, 2008; Streck et al., 2007), but such interaction does not necessarily result in rocks with intermediate Ta/Th values. For example, in the Never Summer Mountains of southern Colorado, mixing between silicic, anatectic melts of mafic Precambrian crust (>70 wt% SiO_2) and ascending mafic melts was likely responsible for the generation of intermediate composition, Oligocene plutonic rocks (Jacob et al., 2015). Both mafic and felsic composition end-members involved in mixing had similar Nd isotopic compositions, ε_{Nd} (T) ~−5, and only small differences in Ta/Th (0.3 vs. 0.2). As a result, mechanical mixing produces little variation in either ε_{Nd} (T) or Ta/Th with increasing wt% SiO_2, characteristics that are indistinguishable from those expected for closed-system magmatic differentiation (Figure 12). Intermediate Ta/Th group basaltic andesites and andesites throughout SWNA also lack a consistent covariation between ε_{Nd} (T) or Ta/Th and wt% SiO_2 (Figures 5 and 12). Even if these rocks were commonly the product of mixing with crustal melts, such mixing would require a mafic end-member with low ε_{Nd} (T) and intermediate Ta/Th values.

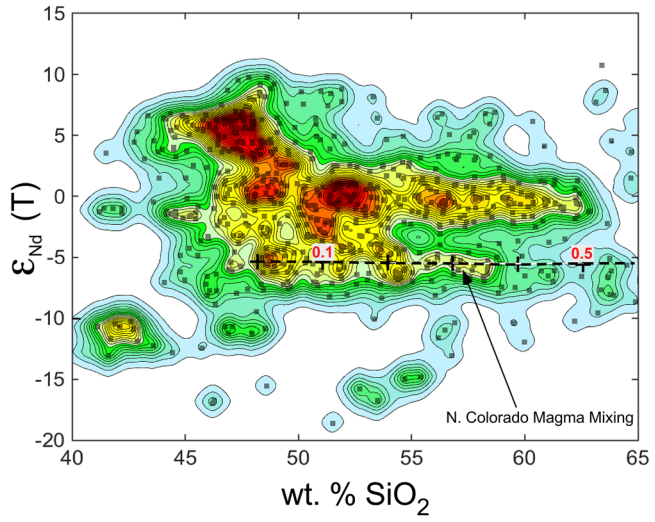

Figure 12. Volcanic rock ε_{Nd} (T) versus wt% SiO_2 (n = 930). Simple mixing line for mafic and felsic melts described in text; labels are fraction of felsic end-member in mixture.

5.2. Role of Crystal-Liquid Separation in Influencing Ta/Th Values

To address whether intermediate Ta/Th values reflect modifications of magmatic Ta/Th values during closed-system differentiation, we turn to the rock ages and compositions from the northern Sierra Nevada and the southern Rio Grande rift. At both locations, the different Ta/Th group rocks are separable by age (Figures 10a and 10d). In the northern Sierra Nevada, low Ta/Th rocks are >10 Ma in age, and intermediate Ta/Th rocks are all <10 Ma (Figure 10d). In the southern Rio Grande rift, volcanism older than 20 Ma produced only intermediate Ta/Th group rocks and <20 Ma volcanism resulted only in rocks of the high Ta/Th group (Figure 10a).

Because the intermediate Ta/Th rocks occur as a separate volcanic event at both locations, we choose to consider the origin and evolution of this magmatism independently of the high or low Ta/Th groups. From this perspective, it is significant that the intermediate Ta/Th rocks at both sites have uncorrelated Ta and Th abundances (Figures 10b and 10e) but have Ta/Th values that are highest and most variable in the most mafic rocks and that decrease with increasing wt% SiO_2 (Figures 10c and 10f). The

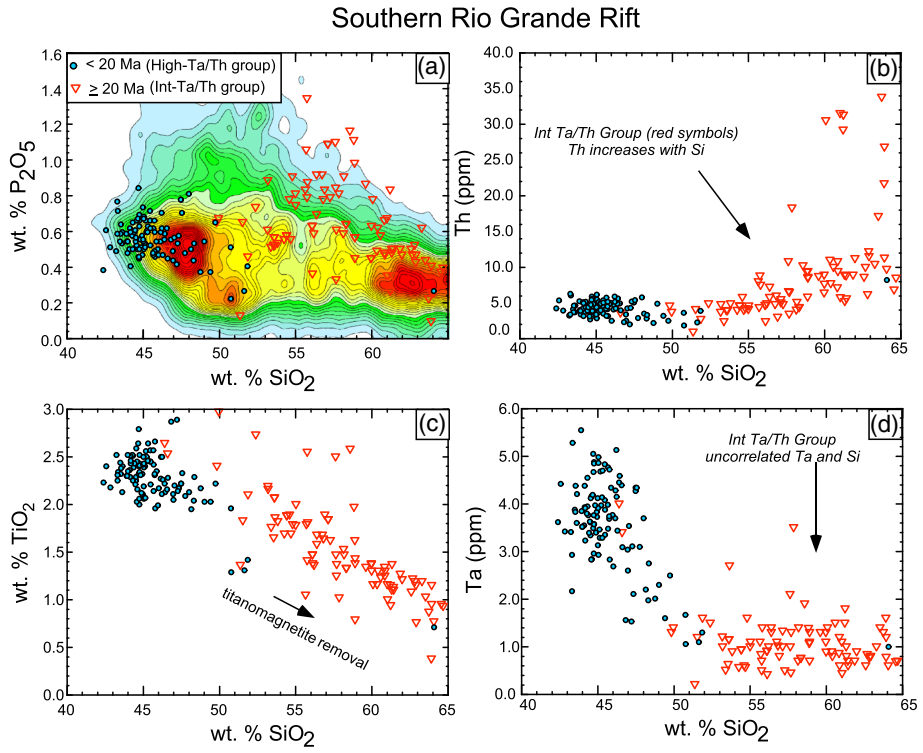

Figure 13. Wt% P_2O_5 (a) Th (ppm) (b) wt% TiO_2 (c) and Ta (ppm) (d) versus for volcanic rocks in southern Rio Grande rift and vicinity.

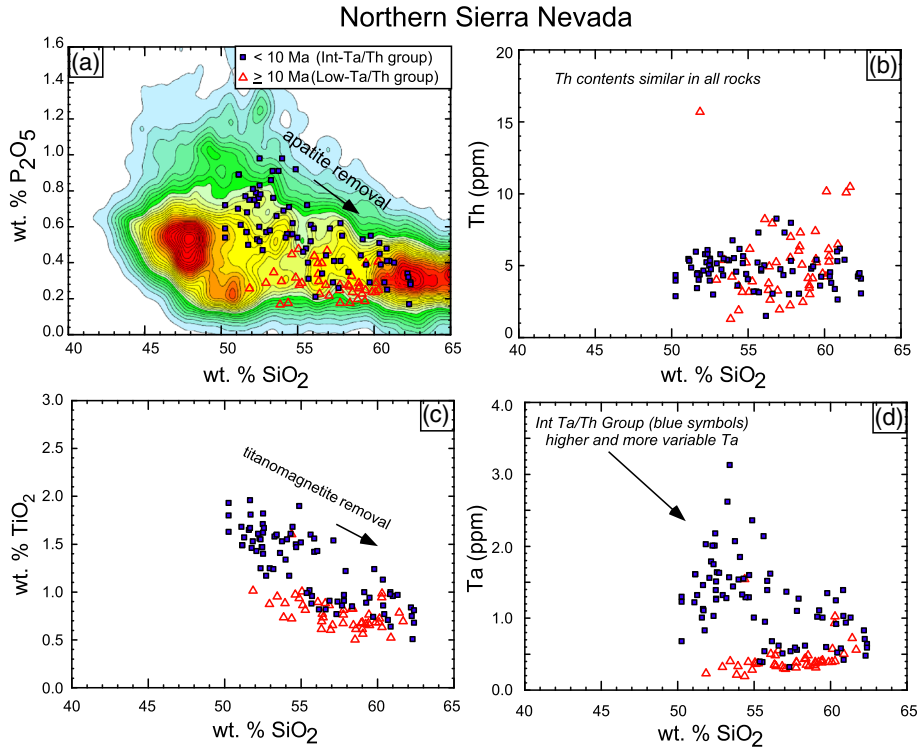

Figure 14. Wt% P_2O_5 (a) Th (ppm) (b) wt% TiO_2 (c) and Ta (ppm) (d) versus for volcanic rocks in northern Sierra Nevada.

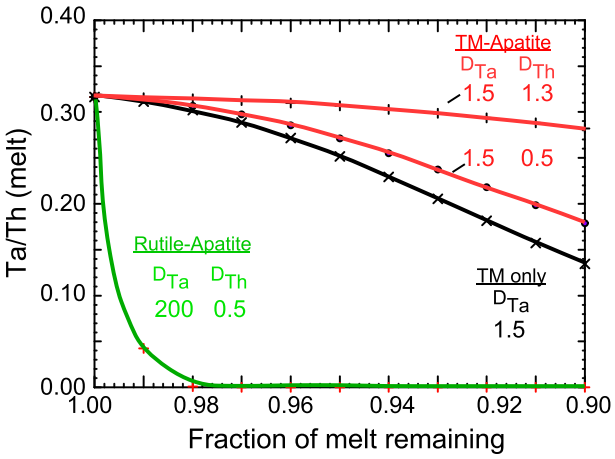

Figure 15. Calculated melt evolution curves illustrating melt Ta/Th values versus fraction of melt remaining during fractionation of rutile, apatite, and/or titanomagnetite from a magma parental to an intermediate Ta/Ta group rock. Starting melt Ta/Th value is average for rocks in northern Sierra Nevada with 50 to 55 wt% SiO_2. Mineral-melt partition coefficients (D) used to calculate fractionation paths are shown in brackets and are in the ranges determined for basaltic andesite melt compositions (Klemme et al., 2005; Prowatke & Klemme, 2006). TM = titanomagnetite.

decrease in Ta/Th values is best explained by crystal-liquid separation from a mafic, intermediate Ta/Th composition magma (Figures 13c, 13d, 14c, and 14d). The lack of a pronounced decrease in Ta abundances with increasing silica (Figures 13d and 14d) precludes the removal of rutile during crystal-liquid separation, but the regular decrease in wt% TiO_2 with increasing wt% SiO_2 (Figures 13c and 14c) is consistent the removal of titanomagnetite, which is found in intermediate Ta/Th group rocks and in which Ta is only weakly compatible (D_{Ta}~1) (Cameron et al., 1989; Nielsen & Beard, 2000). For Th, we note that whole-rock P and Sr contents decrease with increasing silica in the intermediate Ta/Th group rocks, at least in the northern Sierra Nevada, as expected for apatite removal during magmatic differentiation (Figures 14a and S1) (Cousens et al., 2011). Thorium contents remain constant with increasing wt% SiO_2 (Figure 14b) because Th is only weakly compatible in apatite (D_{Th}~1) (Prowatke et al., 2004). In the southern Rio Grande rift, apatite separation apparently did not occur with increasing whole-rock silica, given the lack of a regular decrease in wt% P_2O_5 and the regular increase in Th contents (Figures 13a and 13b).

To illustrate the net effect of titanomagnetite ± apatite ± rutile removal on magma Ta/Th values, we consider fractional crystallization of a mafic melt with intermediate Ta/Th values using a range of Ta and Th mineral-melt partition coefficients pertinent for for these minerals if crystallizing from basaltic andesite melts (Figure 15). With increasing removal of titanomagnetite ± apatite (rutile absent), Ta/Th values decrease by small to moderate amounts at any given fraction of remaining melt, depending on the Th and Ta partition coefficients used. These decreases in Ta/Th values are consistent with the variations in whole-rock Ta/Th values observed with increasing wt% SiO_2 both in the northern Sierra Nevada and the southern Rio Grande rift (Figures 10c and 10f). We conclude that crystal-liquid fractionation affected the Ta/Th values for intermediate Ta/Th groups rocks but is not responsible for their characteristic intermediate and variable Ta/Th values.

5.3. A Mantle Origin for Magmas Parental to Intermediate Ta/Th Group Rocks?

Basaltic andesites in the northern Sierra Nevada and the southern Rio Grande rift are among the least differentiated rocks in the intermediate Th/Th groups, and as a result their high and variable Ta/Th values are likely to represent original characteristics of their parental melts. However, basaltic andesite melts would typically be considered as too silicic to be primary melts of dry peridotite (Kushiro, 2001).

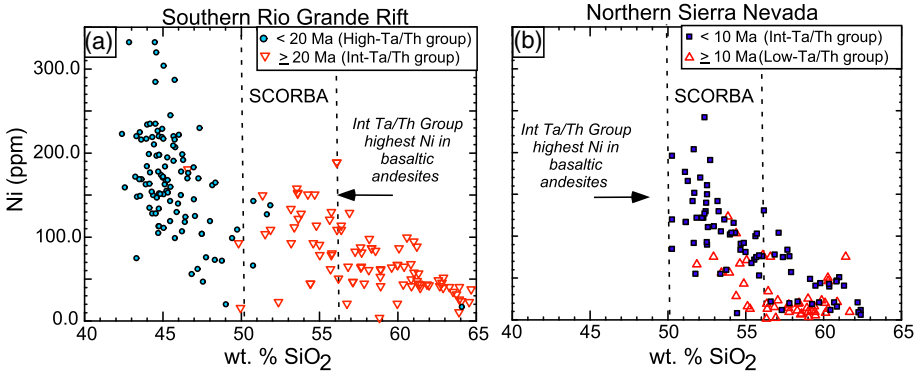

Figure 16. Whole-rock Ni (ppm) versus wt% SiO_2 for volcanic rocks in southern Rio Grande rift (a) and northern Sierra Nevada (b). SCORBA denotes range of wt% SiO_2 for "Southern Cordilleran Basaltic Andesites" (Cameron et al., 1989).

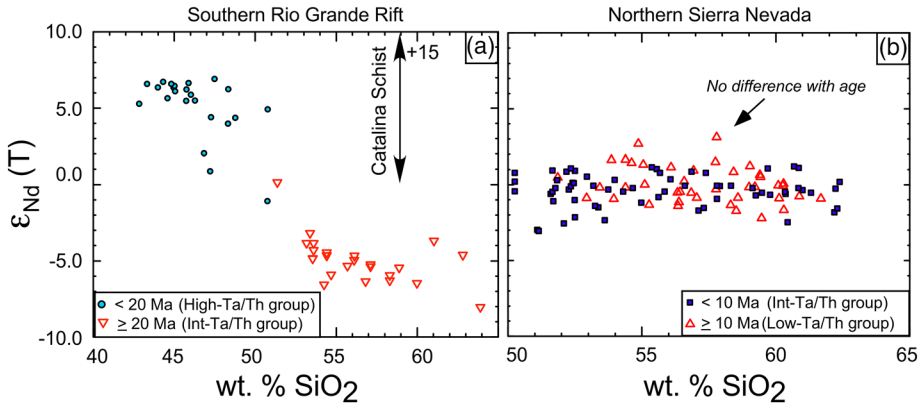

Figure 17. Whole-rock ε_{Nd} (T) versus wt% SiO_2 for volcanic rocks in southern Rio Grande rift (a) and northern Sierra Nevada (b). Range of whole-rock Nd isotopic compositions for Catalina Schist in Late Cretaceous from King et al. (2006).

Previous workers have also recognized this issue, but for a set of Cenozoic "high" wt% MgO (~7), "post-subduction," basaltic andesites found elsewhere in SWNA ("Southern Cordillera Basaltic Andesites", or SCORBA) (Cameron et al., 1989). Based on their high Ni contents (>100 ppm),

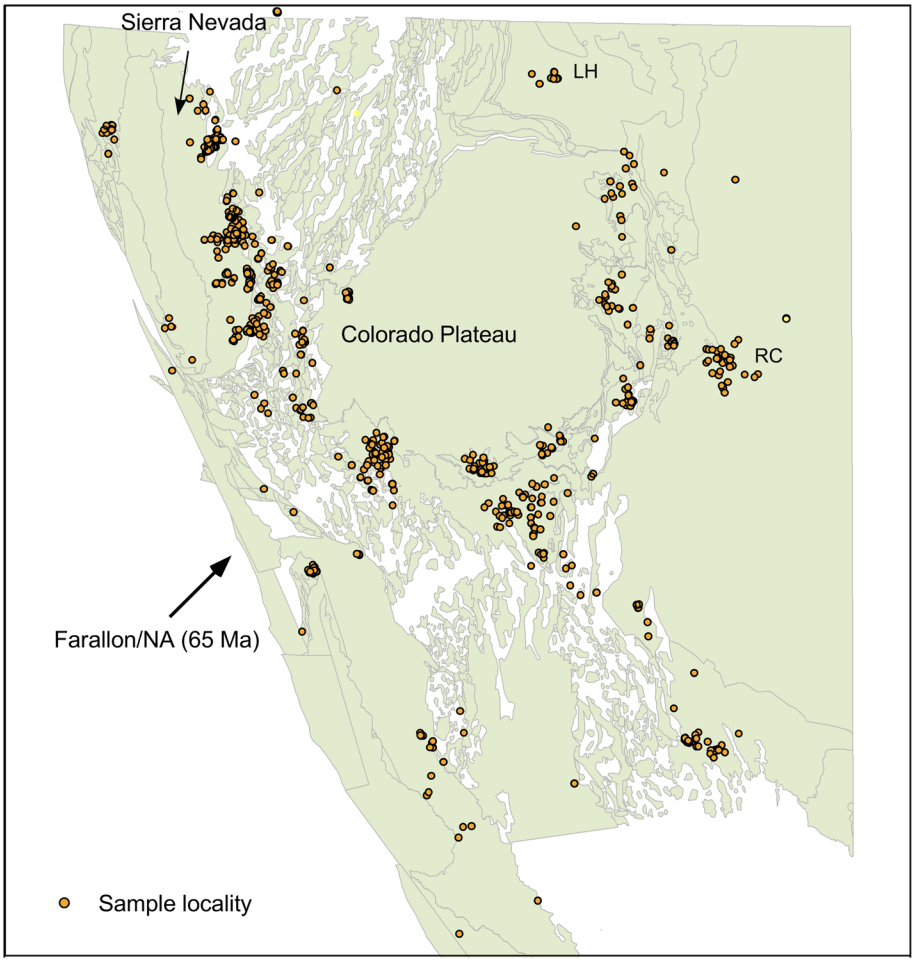

Figure 18. Distribution of intermediate Ta/Th group rocks on palinspastic reconstruction of SWNA at 35 Ma (McQuarrie & Wernicke, 2005). Outlined regions are separate tectonic blocks used in this reconstruction, including the Sierra Nevada block and the Colorado Plateau. RC = Raton-Clayton volcanic field, LH = Leucite Hills. Relative motion of Farallon and North American plates at 65 Ma from Jones et al. (2011).

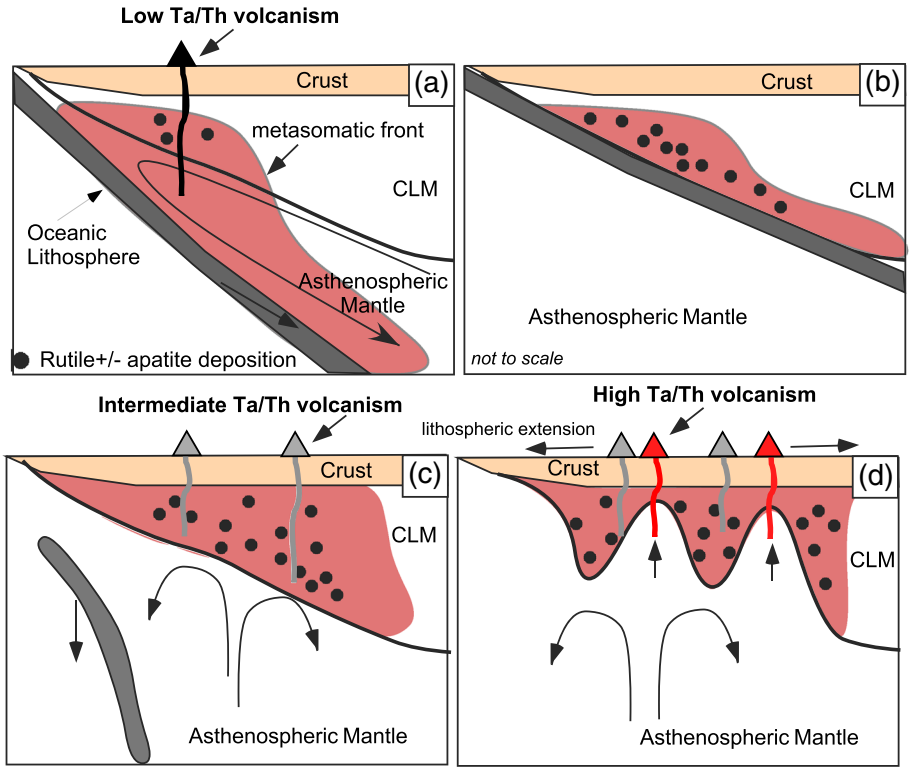

Figure 19. Cartoon showing interplay between infiltrating, subduction-related fluids, and melt generation in continental margin arc (a), lithospheric mantle (c), and upwelling asthenosphere (d). Low-angle subduction can produce widespread metasomatism of mantle lithosphere but does not immediately trigger magmatism due to refrigeration by subducting slab (b).

low CaO/Al_2O_3 (<0.5), and low ε_{Nd} (T) values (<−5), SCORBA volcanic rocks have been interpreted as melts of hydrous, depleted (clinopyroxene-absent), spinel peridotites in the CLM (Lopez & Cameron, 1997), a conclusion consistent with experimental studies of the products of melting of shallow, hydrous mantle (Mitchell & Grove, 2015). The intermediate Ta/Th group basaltic andesites from both the northern Sierra Nevada and southern Rio Grande rift also include rocks with Ni contents greater than 100 ppm (Figures 16a and 16b). In both regions, whole-rock Ni concentrations decrease with increasing wt% SiO_2, presumably as a result of crystal-liquid separation of olivine ± clinopyroxene, the main phenocryst phases found in these rocks (Cousens et al., 2011) (Figures 16a and 16b). We conclude that intermediate Ta/Th group rocks in the northern Sierra Nevada, southern Rio Grande rift, and likely throughout SWNA belong to the SCORBA suite and, as such, represent the products of melting of metasomatized mantle.

As with SCORBA, a CLM source for the intermediate Ta/Th group rocks is consistent with their low ε_{Nd} (T) values, which contrast with high, asthenospheric, ε_{Nd} (T) values for high Ta/Th rocks such as those found in the southern Rio Grande rift (Figures 8, 17a, and 17b). The difference in the Nd isotopic compositions of intermediate Ta/Th rocks in the northern Sierra Nevada and southern Rio Grande reflects the differences in the age and composition of the CLM in these two locations (Cousens et al., 2008; Davis & Hawkesworth, 1993; Farmer et al., 2013).

5.4. Evidence for Apatite ± Rutile in Mantle Source of Intermediate Ta/Th Group Rocks

Intermediate Ta/Th group rocks may owe their unique Ta/Th characteristics to their mantle source regions, but evidence of rutile and/or apatite in the source would best implicate metasomatized CLM in their generation. In fact, the relatively high, but variable, Ti, and Ta concentrations of basaltic andesites in both the northern Sierra Nevada and southern Rio Grande rift are consistent with the dissolution of rutile during

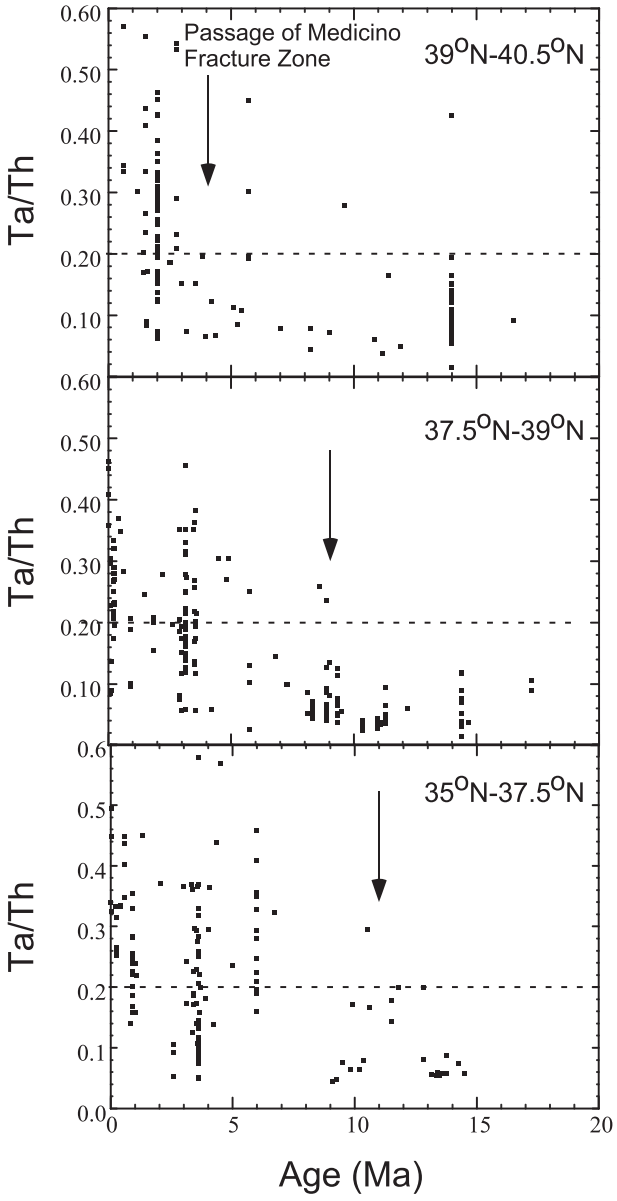

Figure 20. Volcanic rock Ta/Th values as function of age at three different latitudes in western Nevada and eastern California. Approximate timing of passage of Mendocino Fracture Zone at each latitude from Atwater and Stock (1998).

partial mantle melting (Figures 13c, 13d, 14c, and 14d). The variable, and relatively high, P contents (up to 1.2 wt% P_2O_5) of the basaltic andesites (Figures 13a, 13b, 14a, and 14b) are consistent with the consumption of apatite during melting. We note that the basaltic andesites do not have high Th contents, compared to rocks of similar bulk composition in the high or low Ta/Th groups (Figures 13b and 14b), which may be an indication that their CLM sources contained low Th content apatites (<25 ppm), a class of apatites that has been recognized in metasomatized mantle xenoliths at other locations worldwide (O'Reilly & Griffin, 2000).

The above arguments apply to intermediate Ta/Th group rocks throughout SWNA. In the full data set, high Ta/Th rocks cluster at low wt% SiO_2 and wt% P_2O_5 between 0.2 and 0.8 (Figures 13a and 14a). Low Ta/Th rocks form a cluster at higher wt% SiO_2 and lower wt% P_2O_5. Intermediate Ta/Th groups rocks, in contrast, occupy a range of P and Si contents in between the data clusters formed by the other groups that reflects their higher and more variable P contents. Overall, we consider the intermediate Ta/Th group rocks to owe their distinctive Ta/Th values to variable amounts of rutile and apatite in their metasomatized CLM source rocks (Figure 3).

We recognize that previous workers have also proposed a role for high field strength element accessory phases in the sources of CLM-derived volcanic rocks in the SWNA, specifically Fitton et al. (1988) who suggested that the low HFSE/LILE values for these rocks requires a residual high field strength element mineral phase in their metasomatized mantle sources. Our interpretation is similar, but given the high solubility of Ti in mafic composition melts, it is unlikely that Ti-bearing accessory phases could have been preserved in the CLM after melting (Figure 3). Instead, it is more likely that the CLM was sufficiently enriched in LILE relative to HFSE during metasomatism that the resulting low HFSE/LILE values were reflected in the composition of a partial melt even after most of whole-rock budget of HFSE was delivered to that melt (Farmer et al., 2013).

5.5. Distribution of Metasomatized CLM

The widespread geographic distribution of Cenozoic, intermediate Ta/Th volcanic rocks requires that metasomatized CLM must also have been widespread. Using a palinspastic reconstruction of the region at 35 Ma (McQuarrie & Wernicke, 2005), assuming no relative displacement of volcanic rocks and underlying mantle sources during posteruptive lithospheric deformation, the distribution of intermediate Ta/Th rocks suggests that metasomatism extended from beneath the southern Rocky Mountains and adjacent High Plains (Raton-Clayton volcanic field) to at least the southern Wyoming Craton (Leucite Hills; Figure 18). These are all regions that may have been underthrust by the Farallon Plate during the Laramide Orogeny (Saleeby, 2003).

Widespread metasomatism of the CLM during the Laramide Orogeny may also explain why intermediate Ta/Th rocks consistently have higher initial $^{87}Sr/^{86}Sr$ values (0.704 to 0.708) than high Ta/Th basalts (<0.704) (Leeman, 1970) and why the Sr isotopic compositions of intermediate Ta/Th rocks do not vary with the latitude at which they were erupted (Figure 9). The uniformly high $^{87}Sr/^{86}Sr$ values of the intermediate Ta/Th group rocks contrast with their Nd isotopic compositions, which vary with latitude; ε_{Nd} (T) for volcanic rocks are generally >−10 where underlain by Paleoproterozoic lithosphere, to the south, and <−10 where underlain by Archean lithosphere, to the north (Cameron et al., 1989; Lopez & Cameron, 1997; Mirnejad & Bell, 2006) (Figures 1 and 8). The difference between the geographic variability in the Nd and Sr isotopic compositions could stem from the significantly higher mobility of Sr in slab-derived fluids

compared to that of rare earth elements (REE) such as Nd (Porter & White, 2009). As a result, the Sr isotopic composition of metasomatized CLM could reflect that of the Sr mobilized in these fluids, but the Nd isotopic compositions represent that of the Nd indigenous to the Precambrian lithospheric mantle.

We can test this possibility by addressing the range of Sr isotopic compositions possible for slab-derived fluids generated during the Laramide Orogeny. Strontium transported in the metasomatizing fluids was likely sourced in subducting oceanic lithosphere but could not have been derived solely from Sr derived from oceanic crust of the Farallon Plate which had $^{87}Sr/^{86}Sr$ (T) <0.7040 (Sano & Hayasaka, 2004). A potential source of more radiogenic Sr is the tectonic mélange generated in subduction channel beneath SWNA during the Laramide Orogeny. The Catalina Schist exposed in southwestern California, for example, is a metasomatized, physical admixture of accreted continentally derived siliciclastic sediments, oceanic crust, and ultramafic rocks generated during Late Cretaceous subduction along the continental margin (Sorensen & Barton, 1987). These mélanges have high whole-rock ε_{Nd} values (0 to +15; Figure 17a) and experienced a high aqueous fluid flux by fluids in which Sr, but not Nd, was mobile (King et al., 2006). The isotopic compositions of the mobile Sr are more radiogenic than those of the Farallon oceanic crust (initial $^{87}Sr/^{86}Sr$ 0.705 to 0.707; Figure 9) because it contains high $^{87}Sr/^{86}Sr$ Sr from continentally derived sediments as well as low $^{87}Sr/^{86}Sr$ Sr from both mafic and ultramafic rocks. The fluid-mobile Sr isotopic compositions overlap those of the intermediate Th/Th group volcanic rocks, which allow the possibility that fluids derived from underthrust mélange were responsible for metasomatism of the CLM during the Laramide Orogeny throughout SWNA. Further supporting this conclusion is the recent recognition that surface exposures of schists similar in age and composition to the Catalina Schist exist in central Arizona which demonstrates that underthrusting of tectonic mélange during the Laramide Orogeny occurred further inboard than previously appreciated (Jacobson et al., 2017; Strickland & Singleton, 2018).

5.6. Continental Mantle Melt Generation From Ta/Th Values

A critical observation from the southern Rio Grande rift and northern Sierra Nevada is that intermediate Ta/Th group rocks formed during separate volcanic events, either preceded by low Ta/Th volcanism or followed by high Ta/Th volcanism. In the southern Rio Grande rift, all three groups likely formed. Tantalum abundance data do not exist for the Late Cretaceous volcanic rocks in this region, but these rocks have uniformly low Nb/Th values (<1) (McLemore et al., 1999) that are similar to the values for island- and continental-arc volcanic rocks and so belong to the low Ta/Th group. These observations reveal that low, to intermediate, to high Ta/Th group volcanism can occur sequentially in the same geographic area in SWNA, even if over a ~75 million-year time interval.

We consider the regular progression from low, to intermediate, to high Ta/Th volcanism an indication that magmatism in SWNA reflects specific tectonic settings and trigger mechanisms of mantle melting that changed regularly through time (Figure 19). The low Ta/Th rocks are best interpreted as products of continental margin arc volcanism resulting from flux melting in asthenospheric mantle undergoing corner flow during active subduction and dehydration of subducting oceanic lithosphere and overlying tectonic mélange (Figure 19a). Addition of fluids to the mantle wedge directly induces mantle melting but only where the convecting mantle is sufficiently hot to melt when hydrated. Intermediate Ta/Th volcanic rocks are also ultimately the product of mantle melting, but in this case melting of metasomatized CLM. Metasomatism likely occurred in most locations during the Laramide Orogeny, via fluids generated in shallowly subducting oceanic lithosphere that encountered CLM that was maintained at temperatures below the wet peridotite solidus by refrigeration from the underlying oceanic lithosphere, itself (Figures 2a and 19b). The low temperatures inhibited mantle melting but likely enhanced precipitation of accessory mineral phases from the metasomatizing fluids. Melting of the hydrated, rutile ± apatite-bearing CLM occurred as a result of heating by upwelling of asthenosphere triggered either by slab rollback, the removal (sinking) of mantle lithosphere, or the opening of a slabless window (Figure 19c) (Farmer et al., 2008). Sufficient thinning of the lithospheric mantle then allowed for decompression melting of the asthenosphere and the production of high Ta/Th group basalts (Figure 19d) (Daley & DePaolo, 1992; Perry et al., 1987).

Implicit in the above model is that widespread aqueous metasomatism of CLM occurred in the Cenozoic either during subduction associated with the Laramide Orogeny or with Ancestral Cascades volcanism and ultimately accounts for the occurrence of intermediate Ta/Th group rocks throughout SWNA, including the northern Sierra Nevada and the southern Rio Grande rift. However, the onset of intermediate Ta/Th

volcanism may have been triggered in different fashions in any given location. In the southern Rio Grande rift and vicinity, rollback of the shallowing subducting Farallon Plate may have been responsible for intermediate Ta/Th volcanism and for the ignimbrite flare-up, in general (Farmer et al., 2008). In the northern Sierra Nevada, intermediate Ta/Th volcanism only began after the passage of the Mendocino Fracture Zone and opening of slabless window beneath this region (Cousens et al., 2008). A similar transition occurs in volcanic rocks further to south in the Sierra Nevada and adjacent portions of the Great Basin, but the transition occurs at progressively earlier times, mirroring the passage of the Mendocino Fracture Zone as it migrated from south to north (Figure 20) (Putirka & Platt, 2012). This progression can be explained if the Miocene, low Ta/Th volcanism represented localized flux melting of convecting mantle triggered by ascending fluids that interacted with CLM over a much wider area. Melting in the metasomatized CLM was inhibited until opening of a slabless window and upwelling asthenosphere heated the hydrated CLM sufficiently to induce partial melting.

Continental volcanism generated via heating of CLM that was primed for melting by refrigeration from underthrust oceanic lithosphere, and through metasomatism by slab-derived fluids, has been proposed in other regions (Pfänder et al., 2018) and may be a process relevant to the formation of other post-orogenic volcanic rock types (Calmus et al., 2010). However, significant questions remain even in SWNA. For example, low Ta/Th volcanic rocks associated with the Ancestral Cascades in the northern Sierra Nevada have low ε_{Nd} (T) values (Cousens et al., 2008) (Figure 17), which implies that the Nd in these rocks was derived from CLM. If the melts were ultimately generated in the mantle wedge, then these melts must have extensively interacted with and acquired their Nd isotopic composition from the CLM (Navon & Stolper, 1987). Exactly what accounts for the difference in Ta/Th values between low and intermediate group volcanic rocks remains enigmatic considering that both were derived from parental melts that interacted with preexisting CLM.

6. Conclusions

Consideration of the chemical compositions of nearly 2,000 Cenozoic volcanic rock samples from SWNA demonstrates that these rocks can be grouped on the basis of their Ta/Th values. Rocks with low and high Ta/Th values occur both in oceanic settings and in SWNA. In contrast, rocks with intermediate Ta/Th values are common in SWNA but rare among oceanic volcanic rocks. Volcanic rocks comprising the intermediate Ta/Th group are interpreted to be the products of melting of continental lithospheric mantle that had been metasomatized by aqueous fluids during low-angle subduction of oceanic lithosphere that resulted in the deposition of the accessory minerals rutile and apatite. It is the identification of these carrier minerals in the source of the intermediate Ta/Th rocks that most clearly fingerprints the involvement of metasomatized lithospheric mantle in their generation, because these accessory phases are only present in the relatively cool confines of the lithosphere. Additional work will be required to assess whether the compositions of the intermediate Ta/Th group rock can provide insights into other chemical modifications of the CLM that may have accompanied Late Cretaceous to early Cenozoic mantle metasomatism in SWNA.

Acknowledgments
This material is based upon work supported by the National Science Foundation under Grants EAR-0313319, EAR-0622302, and EAR-0607499 (Farmer) and EAR-0312691, EAR-0622313, and EAR-0607499 (Glazner). Jason Ash provided data downloads from NAVDAT, and Craig Jones helped with palinspastic reconstructions. The manuscript was greatly improved by discussions with Marc Norman and by highly constructive journal reviews from Sonja Aulbach, Tyrone Rooney, Cin-Ty Lee, Jörg A. Pfänder, and an anonymous reviewer. The data used for this study are from literature sources and are available through the EarthChem Portal (http://www.earthchem.org/portal).

References

Adam, J., Green, T. H., & Sie, S. H. (1993). Proton microprobe determined partitioning of Rb, Sr, Ba, Y, Zr, Nb and Ta between experimentally produced amphiboles and silicate melts with variable F content. *Chemical Geology*, *109*(1–4), 29–49. https://doi.org/10.1016/0009-2541(93)90060-V

Aiuppa, A., Allard, P., D'Alessandro, W., Michel, A., Parello, F., Treuil, M., & Valenza, M. (2000). Mobility and fluxes of major, minor and trace metals during basalt weathering and groundwater transport at Mt. Etna volcano (Sicily). *Geochimica Et Cosmochimica Acta*, *64*(11), 1827–1841. https://doi.org/10.1016/S0016-7037(00)00345-8

Amato, J. M., Mack, G. H., Jonell, T. N., Seager, W. R., & Upchurch, G. R. (2017). Onset of the Laramide Orogeny and associated magmatism in southern New Mexico based on U-Pb geochronology. *Geological Society of America Bulletin*, *129*(9–10), 1209–1226. https://doi.org/10.1130/B31629.1

Antignano, A., & Manning, C. E. (2008a). Fluorapatite solubility in H_2O and H_2O-NaCl at 700 to 900 degrees C and 0.7 to 2.0 GPa. *Chemical Geology*, *251*(1–4), 112–119. https://doi.org/10.1016/j.chemgeo.2008.03.001

Antignano, A., & Manning, C. E. (2008b). Rutile solubility in H_2O, H_2O-SiO_2, and H_2O-$NaAlSi_3O_8$ fluids at 0.7-2.0 GPa and 700-1000 degrees C: Implications for mobility of nominally insoluble elements. *Chemical Geology*, *255*(1–2), 283–293. https://doi.org/10.1016/j.chemgeo.2008.07.001

Atwater, T., & Stock, J. (1998). Pacific-North America plate tectonics of the Neogene southwestern United States: An update. *International Geology Review*, *40*, 375–402.

Ayers, J. C., & Watson, E. B. (1991). Solubility of apatite, monazite, zircon, and rutile in supercritical aqueous fluids with implications for subduction zone geochemistry. *Philosophical Transactions of the Royal Society of London Series a-Mathematical Physical and Engineering Sciences*, *335*(1638), 365–375. https://doi.org/10.1098/rsta.1991.0052

Baier, J., Audetat, A., & Keppler, H. (2008). The origin of the negative niobium tantalum anomaly in subduction zone magmas. *Earth and Planetary Science Letters*, *267*(1–2), 290–300. https://doi.org/10.1016/j.epsl.2007.11.032

Bailey, E. H., & Ragnarsdottir, K. V. (1994). Uranium and thorium solubilities in subduction zone fluids. *Earth and Planetary Science Letters*, *124*(1-4), 119–129. https://doi.org/10.1016/0012-821x(94)00071-9

Baldridge, W. S., Perry, F. V., Vaniman, D. T., Nealey, L. D., Leavy, B. D., Laughlin, A. W., et al. (1991). Middle to late Cenozoic magmatism of the southeastern Colorado Plateau and Central Rio Grande rift (New Mexico and Arizona, U.S.A.): A model for continental rifting. *Tectonophys.*, *197*, 327–354.

Beard, B. L., & Johnson, C. M. (1997). Hafnium isotope evidence for the origin of Cenozoic basaltic lavas from the southwestern United States. *Journal of Geophysical Research*, *102*, 20,149–120,178.

Bodinier, J. L., Merlet, C., Bedini, R. M., Simien, F., Remaidi, M., & Garrido, C. J. (1996). Distribution of niobium, tantalum, and other highly incompatible trace elements in the lithospheric mantle: The spinel paradox. *Geochem. Cosmochim. Acta*, *60*, 545–550.

Brandon, A. D., Hooper, P. R., Goles, G. G., & Lambert, R. S. (1993). Evaluating crustal contamination in continental basalts—The isotopic composition of the Picture Gorge Basalt of the Columbia River Basalt Group. *Contributions to Mineralogy and Petrology*, *114*(4), 452–464. https://doi.org/10.1007/Bf00321750

Butcher, L. A., Mahan, K. H., & Allaz, J. M. (2017). Late Cretaceous crustal hydration in the Colorado Plateau, USA, from xenolith petrology and monazite geochronology. *Lithosphere*, *L583*, 581–518. https://doi.org/10.1130/L583.1

Calmus, T., Pallares, C., Maury, R. C., Aguillón-Robles, A., Bellon, H., Benoit, M., & Michaud, F. (2010). Volcanic markers of the post-subduction evolution of Baja California and Sonora, Mexico: Slab tearing versus lithospheric rupture of the Gulf of California. *Pure Appl. Geophys*, *168*(8-9), 1303–1330. https://doi.org/10.1007/s00024-010-0204-z

Cameron, K. L., Nimz, G. J., Kuentz, D., Niemeyer, S., & Gunn, S. (1989). The southern Cordilleran basaltic andesite suite, southern Chihuahua, Mexico: A link between Tertiary continental arc and flood basalt magmatism in North America. *Journal of Geophysical Research*, *94*, 7819–7840.

Carlson, R. W., & Nowell, G. M. (2001). Olivine-poor sources for mantle-derived magmas: Os and Hf isotopic evidence from potassic magmas of the Colorado Plateau. *Geochem. Geophys. Geosyst., 2*, 200GC000128.

Chazot, G., Menzies, M. A., & Harte, B. (1996). Determinations of partition coefficients between apatite, clinopyroxene, amphibole, and melt in natural spinel lherzolites from Yemen: Implications for wet melting of the lithospheric mantle. *Geochem. Cosmochim. Acta*, *60*, 423–437.

Christiansen, E. H., & McCurry, M. (2008). Contrasting origins of Cenozoic silicic volcanic rocks from the western Cordillera of the United States. *Bulletin of Volcanology*, *70*(3), 251–267.

Coney, P. J., & Reynolds, S. J. (1977). Cordilleran Benioff zones. *Nature*, *270*(5636), 403–406.

Cousens, B., Prytulak, J., Henry, C., Alcazar, A., & Brownrigg, T. (2008). Geology, geochronology, and geochemistry of the Miocene–Pliocene Ancestral Cascades arc, northern Sierra Nevada, California and Nevada: The roles of the upper mantle, subducting slab, and the Sierra Nevada lithosphere. *Geosphere*, *4*(5), 829. https://doi.org/10.1130/GES00166.1

Cousens, B. L., Henry, C. D., Harvey, B. J., Brownrigg, T., Prytulak, J., & Allan, J. F. (2011). Secular variations in magmatism during a continental arc to post-arc transition: Plio-Pleistocene volcanism in the Lake Tahoe/Truckee area, northern Sierra Nevada, California. *Lithos*, *123*(1–4), 225–242. https://doi.org/10.1016/j.lithos.2010.09.009

Daley, E. E., & DePaolo, D. J. (1992). Isotopic evidence for lithospheric thinning during extension: Southeastern Great Basin. *Geology*, *20*(2), 104–108.

Davis, J., & Hawkesworth, C. (1993). The petrogenesis of 3020 Ma basic and intermediate volcanics from the Mogollon-Datil Volcanic Field, New Mexico, USA. *Contributions to Mineralogy and Petrology*, *115*(2), 165–183.

DePaolo, D. J., & Daley, E. E. (2000). Neodymium isotopes in basalts of the southwest Basin and Range and lithospheric thinning during continental extension. *Chemical Geology*, *169*(1–2), 157–185.

Dickinson, W. R. (2004). Evolution of the North American Cordillera. https://doi.org/10.1146/annurev.earth.32.101802.120257.

Dumitru, T. A., Gans, P. B., Foster, D. A., & Miller, E. L. (1991). Refrigeration of the western Cordilleran lithosphere during Laramide shallow-angle subduction. *Geology*, *19*(11), 1145–1148.

Eilers, P. H. C., & Goeman, J. J. (2004). Enhancing scatterplots with smoothed densities. *Bioinformatics*, *20*(5), 623–628. https://doi.org/10.1093/bioinformatics/btg454

Elston, W. E., Damon, P. E., Coney, P. J., Rhodes, R. C., Smith, E. I., & Bikerman, M. (1973). Tertiary volcanic-vocks, Mogollon-Datil Province, New Mexico, and surrounding region: K-Ar dates, patterns of eruption, and periods of mineralization. *Geological Society of America Bulletin*, *84*(7), 2259.

English, J. M., & Johnston, S. T. (2004). The Laramide Orogeny: What were the driving forces? *International Geology Review*, *46*(9), 833–838. https://doi.org/10.2747/0020-6814.46.9.833

Farmer, G. L. 2003. Continental basaltic rocks. In R. L. Rudnick (Eds.). *The Crust* (Vol. 3, pp. 85–121). Elsevier Sci., New York: Elsevier.

Farmer, G. L., Bailley, T., & Elkins-Tanton, L. T. (2008). Mantle source volumes and the origin of the mid-Tertiary ignimbrite flare-up in the southern Rocky Mountains, western US. *Lithos*, *102*(1–2), 279–294.

Farmer, G. L., Glazner, A. F., Kortemeier, W. T., Cosca, M. A., Jones, C. H., Moore, J. E., & Schweickert, R. A. (2013). Mantle lithosphere as a source of postsubduction magmatism, northern Sierra Nevada, California. *Geosphere*, *9*(5), 1102–1124. https://doi.org/10.1130/Ges00885.1

Farmer, G. L., Glazner, A. F., & Manley, C. R. (2002). Did lithospheric delamination trigger late Cenozoic potassic volcanism in the southern Sierra Nevada, California? *Geol. Soc. Amer. Bull.*, *114*, 754–768.

Farmer, G. L., Glazner, A. F., Wilshire, H. G., Wooden, J. L., Pickthorn, W. J., & Katz, M. (1995). Origin of late Cenozoic basalts at the Cima volcanic field, Mojave Desert, California. *J. Geophys. Res.*, *100*, 8399–8415.

Fitton, J. G., Dodie, J., & Leeman, W. P. (1991). Basic magmatism associated with late Cenozoic extension in the Western United States: Compositional variations in space and time. *Journal of Geophysical Research*, *96*, 13,693–613,711.

Fitton, J. G., James, D., Kempton, P. D., Ormerod, D. S., & Leeman, W. P. (1988). The role of lithospheric mantle in the generation of late Cenozoic basic magmas in the western United States. *J. Petrol., Spec. Lithosphere Issue*, 331–349.

Fitzpayne, A., Giuliani, A., Harris, C., Thomassot, E., Cheng, C., & Hergt, J. (2019). Evidence for subduction-related signatures in the southern African lithosphere from the N-O isotopic composition of metasomatic mantle minerals. *Geochimica et Cosmochimica Acta*, *266*, 237–257. https://doi.org/10.1016/j.gca.2019.02.037

Furman, T., & Graham, D. (1999). Erosion of lithospheric mantle beneath the East African rift system: Geochemical evidence from the Kivu volcanic province. *Lithos*, *48*, 237–262.

Gaetani, G. A., Asimow, P. D., & Stolper, E. M. (2008). A model for rutile saturation in silicate melts with applications to eclogite partial melting in subduction zones and mantle plumes. *Earth and Planetary Science Letters*, *272*(3–4), 720–729. https://doi.org/10.1016/j.epsl.2008.06.002

Glazner, A. F., & Farmer, G. L. (1992). Production of isotopic variability in continental basalts by cryptic crustal contamination. *Science*, *255*, 72–74.

Glazner, A. F., & Ussler, W. (1989). Crustal extension, crustal density, and the evolution of Cenozoic magmatism in the Basin and Range of the western United States. *Journal of Geophysical Research*, *94*, 7950–7960.

Hanson, G. N. (1989). An approach to trace element modeling using a simple igneous system. *Reviews in Mineralogy and Geochemistry*, *21*(1), 79–97.

Hauri, E. H., Wagner, T. P., & Grove, T. L. (1994). Experimental and natural partitioning of Th, U, Pb and other trace-elements between garnet, clinopyroxene and basaltic melts. *Chemical Geology*, *117*(1–4), 149–166.

Hickson, C. J., & Juras, S. J. (1986). Sample contamination by grinding. *Canadian Mineralogist*, *24*, 585–589.

Hirschmann, M. M. (2000). Mantle solidus: Experimental constraints and the effect of peridotite composition. *G3*, 1. https://doi.org/10.1029/2000GC000070

Humphreys, E., Hessler, E., Dueker, K., Farmer, G. L., Erslev, E., & Atwater, T. (2003). How Laramide-age hydration of North American lithosphere by the Farallon slab controlled subsequent activity in the western United States. *International Geology Review*, *45*(7), 575–595.

Ionov, D. A. (2010). Petrology of mantle wedge lithosphere: New data on supra-subduction zone peridotite xenoliths from the andesitic Avacha Volcano, Kamchatka. *Journal of Petrology*, *51*(1–2), 327–361. https://doi.org/10.1093/petrology/egp090

Ionov, D. A., & Hofmann, A. W. (1995). Nb-Ta-rich mantle amphiboles and micas—Implications for subduction-related metasomatic trace-element fractionations. *Earth and Planetary Science Letters*, *131*(3-4), 341–356. https://doi.org/10.1016/0012-821x(95)00037-D

Jacob, K. H., Farmer, G. L., Buchwaldt, R., & Bowring, S. A. (2015). Deep crustal anatexis, magma mixing, and the generation of epizonal plutons in the southern Rocky Mountains, Colorado. *Contributions to Mineralogy and Petrology, 169*(1). https://doi.org/10.1007/s00410-014-1094-3

Jacobson, C. E., Hourigan, J. K., Haxel, G. B., & Grove, M. (2017). Extreme latest Cretaceous-Paleogene low-angle subduction: Zircon ages from Orocopia Schist at Cemetery Ridge, southwestern Arizona, USA. *Geology*, *45*(10), 951–954. https://doi.org/10.1130/G39278.1

James, E. W., & Henry, C. D. (1991). Compositional changes in Trans-Pecos Texas magmatism coincident with Cenozoic stress realignment. *Journal of Geophysical Research-Solid Earth and Planets*, *96*(B8), 13,561–13,575. https://doi.org/10.1029/91jb00203

John, D. A., du Bray, E. A., Blakely, R. J., Fleck, R. J., Vikre, P. G., Box, S. E., & Moring, B. C. (2012). Miocene magmatism in the Bodie Hills volcanic field, California and Nevada: A long-lived eruptive center in the southern segment of the Ancestral Cascades arc. *Geosphere*, *8*(1), 44–97. https://doi.org/10.1130/Ges00674.1

Johnson, J. S., Gibson, S. A., Thompson, R. N., & Nowell, G. M. (2005). Volcanism in the Vitim Volcanic Field, Siberia: Geochemical evidence for a mantle plume beneath the Baikal Rift zone. *Journal of Petrology*, *46*(7), 1309–1344.

Jones, C. H., Farmer, G. L., Sageman, B., & Zhong, S. (2011). Hydrodynamic mechanism for the Laramide Orogeny. *Geosphere*, *7*(1), 183–201. https://doi.org/10.1130/GES00575.S1

Kalfoun, F., Ionov, D., & Merlet, C. (2002). HFSE residence and Nb/Ta ratios in metasomatised, rutile-bearing mantle peridotites. *Earth and Planetary Science Letters*, *199*(1–2), 49–65.

Kelemen, P. B., Hanghøj, K., & Greene, A. R. (2014). One view of the geochemistry of subduction-related magmatic arcs, with an emphasis on primitive andesite and lower crust. In R. L. Rudnick (Eds.). *The Crust* (2nd ed., vol. 3, pp. 749–806). Elsevier Sci., New York: Elsevier.

King, R. L., Bebout, G. E., Moriguti, T., & Nakamura, E. (2006). Elemental mixing systematics and Sr-Nd isotope geochemistry of melange formation: Obstacles to identification of fluid sources to arc volcanics. *Earth and Planetary Science Letters*, *246*(3–4), 288–304. https://doi.org/10.1016/j.epsl.2006.03.053

Kistler, R. W., & Peterman, Z. E. (1973). Variations in Sr, Rb, K, Na, and initial Sr-87-Sr-86 in Mesozoic granitic rocks and intruded wall rocks in central California. *Geological Society of America Bulletin*, *84*(11), 3489–3511. https://doi.org/10.1130/0016-7606(1973)84<3489:Visrkn>2.0.Co;2

Klemme, S., Prowatke, S., Hametner, K., & Gunther, D. (2005). Partitioning of trace elements between rutile and silicate melts: Implications for subduction zones. *Geochimica et Cosmochimica Acta*, *69*(9), 2361–2371. https://doi.org/10.1016/j.gca.2004.11.015

Konzett, J., & Frost, D. J. (2009). The high P-T stability of hydroxyl-apatite in natural and simplified MORB—An experimental study to 15 GPa with implications for transport and storage of phosphorus and halogens in subduction zones. *Journal of Petrology*, *50*(11), 2043–2062. https://doi.org/10.1093/petrology/egp068

Kurtz, A. C., Derry, L. A., Chadwick, O. A., & Alfano, M. J. (2000). Refractory element mobility in volcanic soils. *Geology*, *28*(8), 683–686. https://doi.org/10.1130/0091-7613(2000)28<683:Remivs>2.0.Co;2

Kushiro, I. (2001). Partial melting experiments on peridotite and origin of mid-ocean ridge basalt. *Annual Review of Earth and Planetary Sciences*, *29*, 71–107.

Lawton, T. F., & McMillan, N. J. (1999). Arc abandonment as a cause for passive continental rifting: Comparison of the Jurassic Mexican Borderland rift and the Cenozoic Rio Grande rift. *Geology*, *27*(9), 779–782.

Lee, C. T. A. (2005). Trace element evidence for hydrous metasomatism at the base of the North American lithosphere and possible association with Laramide low-angle subduction. *Journal of Geology*, *113*(6), 673–685.

Leeman, W. P. (1970). The isotopic composition of strontium in late Cenozoic basalts from the Basin and Range province, western U.S.A. *Geochim. Cosmochim. Acta*, *34*, 857–872.

Leeman, W. P., & Rogers, J. J. W. (1970). Late Cenozoic alkali-olivine basalts of Basin-Range Province, USA. *Contributions to Mineralogy and Petrology*, *25*(1), 1. https://doi.org/10.1007/Bf00383059

Li, Z.-X. A., Lee, C.-T. A., Peslier, A. H., Lenardic, A., & Mackwell, S. J. (2008). Water contents in mantle xenoliths from the Colorado Plateau and vicinity: Implications for the mantle rheology and hydration-induced thinning of continental lithosphere. *Journal of Geophysical Research*, *113*(B9), B09210. https://doi.org/10.1029/2007JB005540

Lipman, P. W., Prostka, H. J., & Christiansen, R. L. (1971). Evolving subduction zones in the western United States, as interpreted from igneous rocks. *Science*, *174*(4011), 821–825. https://doi.org/10.1126/science.174.4011.821

Lipman, P. W., Prostka, H. J., & Christiansen, R. L. (1972). Cenozoic volcanism and plate-tectonic evolution of the western United States; I, Early and middle Cenozoic. *Phil. Trans. Roy. Soc. Lond., Series A*, *271*, 217–248.

Lopez, R., & Cameron, K. L. (1997). High-Mg andesites from the Gila Bend Mountains, southwestern Arizona: Evidence for hydrous melting of lithosphere during Miocene extension. *Geol. Soc. Amer. Bull.*, *109*, 900–914.
Mair, P., Tropper, P., Harlov, D. E., & Manning, C. E. (2017). The solubility of apatite in H_2O, KCl-H_2O, NaCl-H_2O at 800 degrees C and 1.0 GPa: Implications for REE mobility in high-grade saline brines. *Chemical Geology*, *470*, 180–192. https://doi.org/10.1016/j.chemgeo.2017.09.015
McDonough, W. F., Stosch, H. G., & Ware, N. G. (1992). Distribution of titanium and the rare-earth elements between peridotitic minerals. *Contributions to Mineralogy and Petrology*, *110*(2–3), 321–328. https://doi.org/10.1007/BF00310747
McLemore, V. T., Munroe, E. A., Heizler, M. T., & McKee, C. (1999). Geochemistry of the Copper Flat porphyry and associated deposits in the Hillsboro mining district, Sierra County, New Mexico, USA. *Journal of Geochemical Exploration*, *67*(1–3), 167–189. https://doi.org/10.1016/S0375-6742(99)00072-2
McQuarrie, N., & Wernicke, B. P. (2005). An animated tectonic reconstruction of southwestern North America since 36 Ma. *Geosphere*, *1*(3), 147–172. https://doi.org/10.1130/Ges00016.1
Menzies, M., Kempton, P., & Dungan, M. (1985). Interaction of continental lithosphere and asthenospheric melts below the Geronimo volcanic field, Arizona, U.S.A. *Journal of Petrology*, *26*, 663–693.
Mirnejad, H., & Bell, K. (2006). Origin and source evolution of the Leucite Hills lamproites: Evidence from Sr-Nd-Pb-O isotopic compositions. *Journal of Petrology*, *47*(12), 2463–2489. https://doi.org/10.1093/petrology/egl051
Mitchell, A. L., & Grove, T. L. (2015). Melting the hydrous, subarc mantle: The origin of primitive andesites. *Contributions to Mineralogy and Petrology*, *170*(2), 1–23. https://doi.org/10.1007/s00410-015-1161-4
Mysen, B. O., & Boettcher, A. L. (1975). Melting of a hydrous mantle.1. Phase relations of natural peridotite at high-pressures and temperatures with controlled activities of water, carbon-dioxide, and hydrogen. *Journal of Petrology*, *16*(3), 520–548.
Navon, O., & Stolper, E. (1987). Geochemical consequences of melt percolation—The upper mantle as a chromatographic column. *Journal of Geology, 95*(3), 285–307. https://doi.org/10.1086/629131.
Nielsen, R. L., & Beard, J. S. (2000). Magnetite-melt HFSE partitioning. *Chemical Geology*, *164*(1–2), 21–34. https://doi.org/10.1016/S0009-2541(99)00139-4
Nielsen, S. G., & Marschall, H. R. (2017). Geochemical evidence for melange melting in global arcs. *Science Advances, 3*(4). doi: UNSP e1602402 https://doi.org/10.1126/sciadv.1602402.
Nielson, J. E., Budahn, J. R., Unruh, D. M., & Wilshire, H. G. (1993). Actualistic models of mantle metasomatism documented in a composite xenolith from Dish Hill, California. *Geochim. Cosmochim. Acta*, *57*, 105–121.
O'Reilly, S. Y., & Griffin, W. L. (2013). Mantle metasomatism. In D. E. Harlov, & J. Austrheim (Eds.), *Metasomatism and the chemical transformation of rock*, (pp. 471–534). Heidelberg: Springer.
O'Hara, M. J., Fry, N., & Prichard, H. M. (2001a). Minor phases as carriers of trace elements in non-modal crystal-liquid separation processes I: Basic relationships. *Journal of Petrology*, *42*(10), 1869–1885. https://doi.org/10.1093/petrology/42.10.1869
O'Hara, M. J., Fry, N., & Prichard, H. M. (2001b). Minor phases as carriers of trace elements in non-modal crystal-liquid separation processes II: Illustrations and bearing on behaviour of REE, U, Th and the PGE in igneous processes. *Journal of Petrology*, *42*(10), 1887–1910.
O'Reilly, S. Y., & Griffin, W. L. (2000). Apatite in the mantle: Implications for metasomatic processes and high heat production in Phanerozoic mantle. *Lithos*, *53*, 217–232.
Padilla, A. J., & Gualda, G. A. R. (2016). Crystal-melt elemental partitioning in silicic magmatic systems: An example from the Peach Spring Tuff high-silica rhyolite, Southwest USA. *Chemical Geology*, *440*, 326–344. https://doi.org/10.1016/j.chemgeo.2016.07.004
Perry, F. V., Baldridge, W. S., & DePaolo, D. J. (1987). Role of asthenosphere and lithosphere in the genesis of late Cenozoic basaltic rocks from the Rio Grande rift and adjacent regions of the southwestern United States. *Journal of Geophysical Research*, *92*, 9193–9213.
Pfänder, J. A., Jung, S., Klugel, A., Munker, C., Romer, R. L., Sperner, B., & Rohrmuller, J. (2018). Recurrent local melting of metasomatised lithospheric mantle in response to continental rifting: Constraints from basanites and nephelinites/melilitites from SE Germany. *Journal of Petrology*, *59*(4), 667–694. https://doi.org/10.1093/petrology/egy041
Plank, T., & Langmuir, C. H. (1993). Tracing trace-elements from sediment input to volcanic output at subduction zones. *Nature*, *362*(6422), 739–743. https://doi.org/10.1038/362739a0
Porter, K. A., & White, W. M. (2009). Deep mantle subduction flux. *Geochemistry, Geophysics, Geosystems*, *10*(12), Q12016. https://doi.org/10.1029/2009GC002656
Potts, P. J. (1997). Geoanalysis: Past, present and future. *Analyst*, *122*(11), 1179–1186. https://doi.org/10.1039/a704856d
Prowatke, S., & Klemme, S. (2006). Trace element partitioning between apatite and silicate melts. *Geochimica et Cosmochimica Acta*, *70*(17), 4513–4527. https://doi.org/10.1016/j.gca.2006.06.162
Prowatke, S., Klemme, S., & Ludwig, T. (2004). Experimental constraints on the partitioning of trace elements between apatite and silicate melts. *Lithos*, *73*(1–2), S91–S91.
Putirka, K., & Platt, B. (2012). Basin and Range volcanism as a passive response to extensional tectonics. *Geosphere*, *8*(6), 1274–1285. https://doi.org/10.1130/Ges00803.1
Rooney, T. O., Nelson, W. R., Ayalew, D., Hanan, B., Yirgu, G., & Kappelman, J. (2017). Melting the lithosphere: Metasomes as a source for mantle-derived magmas. *Earth and Planetary Science Letters*, *461*, 105–118. https://doi.org/10.1016/j.eps1.2016.12.010
Rudnick, R. L., & Gao, S. (2003). The composition of the continental crust. In R. L. Rudnick (Eds.). *The Crust* (Vol. 3, pp. 1–64). Elsevier Sci., New York: Elsevier.
Ryerson, F. J., & Watson, E. B. (1987). Rutile saturation in magma: Implications for Ti-Nb-Ta depletion in island-arc basalts. *Earth and Planetary Science Letters*, *86*, 225–239.
Saleeby, J. (2003). Segmentation of the Laramide slab—Evidence from the southern Sierra Nevada region. *Geological Society of America Bulletin*, *115*(6), 655–668.
Sano, S., & Hayasaka, Y. (2004). Sr and Nd geochemistry of Hole 1179D basalts. In W. W. Sager, T. Kanazawa, & C. Escutia (Eds.), *Proc. ODP, sci. results* (Vol. 191, pp. 1–11). College Station TX: Ocean Drilling Program.
Schaffer, L. A., Peslier, A. H., Brandon, A. D., Bizimis, M., Gibler, R., Norman, M., & Harvey, J. (2019). Effects of melting, subduction-related metasomatism, and sub-solidus equilibration on the distribution of water contents in the mantle beneath the Rio Grande rift. *Geochimica et Cosmochimica Acta*, *266*, 351–381. https://doi.org/10.1016/j.gca.2018.10.005
Schmidt, K. H., Botazzi, P., Vannucci, R., & Mengel, K. (1999). Trace element partitioning between phlogopite, clinopyroxene and leucite lamproite melt. *Earth and Planetary Science Letters*, *168*, 287–299.
Smith, D. (2010). Antigorite peridotite, metaserpentinite, and other inclusions within diatremes on the Colorado Plateau, SW USA: Implications for the mantle wedge during low-angle subduction. *Journal of Petrology*, *51*(6), 1355–1379. https://doi.org/10.1093/petrology/egq022

Smith, D., & Griffin, W. L. (2005). Garnetite xenoliths and mantle-water interactions below the Colorado Plateau, southwestern United States. *Journal of Petrology*, *46*(9), 1901–1924.
Smith, J. V. (1981). Halogen and phosphorus storage in the Earth. *Nature*, *289*(5800), 762–765. https://doi.org/10.1038/289762a0
Snyder, W. S., Dickinson, W. R., & Silberman, M. L. (1976). Tectonic implications of space-time patterns of Cenozoic magmatism in western United States. *Earth and Planetary Science Letters*, *32*(1), 91–106.
Sorensen, S. S., & Barton, M. D. (1987). Metasomatism and partial melting in a subduction complex Catalina Schist, Southern California. *Geology*, *15*(2), 115–118. https://doi.org/10.1130/0091-7613(1987)15<115:Mapmia>2.0.Co;2
Streck, M. J., Leeman, W. P., & Chesley, J. (2007). High-magnesian andesite from Mount Shasta: A product of magma mixing and contamination, not a primitive mantle melt. *Geology*, *35*(4), 351–354. https://doi.org/10.1130/G23286a.1
Strickland, E. D., & Singleton, J. S. (2018). Multistage exhumation of Orocopia Schist at the northern Plomosa Mountains Metamorphic Core Complex, west-central Arizona. *Geological Society of America Abstracts Programs*, *50*(5). https://doi.org/10.1130/abs/2018RM-313718
Tang, M., Lee, C. T. A., Chen, K., Erdman, M., Costin, G., & Jiang, H. H. (2019). Nb/Ta systematics in arc magma differentiation and the role of arclogites in continent formation. *Nature Communications*, *10*, ARTN 235. https://doi.org/10.1038/s41467-018-08198-3
Tanis, E. A., Simon, A., Zhang, Y., Chow, P., Xiao, Y., Hanchar, J. M., et al. (2016). Rutile solubility in NaF-NaCl-KCl-bearing aqueous fluids at 0.52.79 GPa and 250650 degrees C. *Geochimica et Cosmochimica Acta*, *177*, 170–181. https://doi.org/10.1016/j.gca.2016.01.003
Walker, J. D., Bowers, T. D., Black, R. A., Glazner, A. F., Farmer, G. L., & Carlson, R. W. (2006). A geochemical database for western North American volcanic and intrusive rocks (NAVDAT). *Special Paper - Geological Society of America*, *397*, 61–71.
Walter, M. J. (1998). Melting of garnet peridotite and the origin of komatiite and depleted lithosphere. *Journal of Petrology*, *39*, 29–60.
Wang, L. P., Essene, E. J., & Zhang, Y. X. (1999). Mineral inclusions in pyrope crystals from Garnet Ridge, Arizona, USA: Implications for processes in the upper mantle. *Contributions to Mineralogy and Petrology*, *135*(2-3), 164–178. https://doi.org/10.1007/s004100050504
Watson, E. B. (1980). Apatite and phosphorus in mantle source regions: An experimental study of apatite/melt equilibria at pressures to 25 kbar. *Earth and Planetary Science Letters*, *51*(2), 322–335.
White, W. M. (2015). Probing the Earth's deep interior through geochemistry. *Geochemical Perspectives*, *4*(2), 95–251. https://doi.org/10.7185/geochempersp.4.2
Whitmeyer, S. J., & Karlstrom, K. E. (2007). Tectonic model for the Proterozoic growth of North America. *Geosphere*, *3*(4), 220–259. https://doi.org/10.1130/GES00055.S1
Wilshire, H. G., Meyer, C. E., Nakata, J. K., Calk, L. C., Shervais, J. W., Nielson, J. E., & Schwarzman, E. C. (1988). Mafic and ultramafic xenoliths from volcanic rocks of the western United States (Vol. *1443*).
Zheng, Y. F. (2019). Subduction zone geochemistry. *Geoscience Frontiers*, *10*(4), 1223–1254. https://doi.org/10.1016/j.gsf.2019.02.003

References From the Supporting Information

Aguillón-Robles, A., Calmus, T., Benoit, M., Bellon, H., Maury, R. C., Cotten, J., et al. (2001). Late Miocene adakites and Nb-enriched basalts from Vizcaino Peninsula, Mexico: Indicators of East Pacific Rise subduction below southern Baja California? *Geol*, *29*(6), 531.
Benoit, M., Aguillon-Robles, A., Calmus, T., Maury, R. C., Bellon, H., Cotten, J., et al. (2002). Geochemical diversity of Late Miocene volcanism in southern Baja California, Mexico: Implication of mantle and crustal sources during the opening of an asthenospheric window. *Journal of Geology*, *110*(6), 627–648.
Cortés, J. A., Smith, E. I., Valentine, G. A., Johnsen, R., Rasoazanamparany, C., Widom, E., et al. (2015). Intrinsic conditions of magma genesis at the Lunar Crater Volcanic Field (Nevada), and implications for internal plumbing and magma ascent. *American Mineralogist*, *100*(2–3), 396–413. https://doi.org/10.2138/am-2015-4812
Cousens, B., Wetmore, S., & Henry, C. D. (2013). The Pliocene-Quaternary Buffalo Valley volcanic field, Nevada: Post-extension, intraplate magmatism in the north-central Great Basin, USA. *Journal of Volcanology and Geothermal Research*, *268*, 17–35. https://doi.org/10.1016/j.jvolgeores.2013.10.006
Ferrari, L., Lopez-Martinez, M., Orozco-Esquivel, T., Bryan, S. E., Duque-Trujillo, J., Lonsdale, P., & Solari, L. (2013). Late Oligocene to Middle Miocene rifting and synextensional magmatism in the southwestern Sierra Madre Occidental, Mexico: The beginning of the Gulf of California rift. *Geosphere*, *9*(5), 1161–1200. https://doi.org/10.1130/Ges00925.1
González-León, C. M., Solari, L., Solé, J., Ducea, M. N., Lawton, T. F., Bernal, J. P., et al. (2011). Stratigraphy, geochronology, and geochemistry of the Laramide magmatic arc in north-central Sonora, Mexico. *Geosphere*, *7*(6), 1392–1418. https://doi.org/10.1130/Ges00679.1
Herzig, C. T., & Jacobs, D. C. (1994). Cenozoic volcanism and 2-state extension in the Salton Trough, Southern California and Northern Baja California. *Geology*, *22*(11), 991–994. https://doi.org/10.1130/0091-7613(1994)022<0991:Cvatse>2.3.Co;2
Konstantinou, A., Valley, J., Strickland, A., Miller, E. L., Fisher, C., Vervoort, J., & Wooden, J. (2013). Geochemistry and geochronology of the Jim Sage volcanic suite, southern Idaho: Implications for Snake River Plain magmatism and its role in the history of Basin and Range extension. *Geosphere*, *9*(6), 1681–1703. https://doi.org/10.1130/Ges00948.1
Lynch, D. J., Musselman, T. E., Gutmann, J. T., & Patchett, P. J. (1993). Isotopic evidence for the origin of Cenozoic volcanic-rocks in the Pinacate Volcanic Field, northwestern Mexico. *Lithos*, *29*(3-4), 295–302. https://doi.org/10.1016/0024-4937(93)90023-6
McDowell, S. M., Overton, S., Fisher, C. M., Frazier, W. O., Miller, C. F., Miller, J. S., & Economos, R. C. (2016). Hafnium, oxygen, neodymium, strontium, and lead isotopic constraints on magmatic evolution of the supereruptive southern Black Mountains volcanic center, Arizona, U.S.A.: A combined LASS zircon-whole-rock study. *American Mineralogist*, *101*, 311–327.
Moreno, F. A. P., & Demant, A. (1999). The Recent Isla San Luis volcanic centre: Petrology of a rift-related volcanic suite in the northern Gulf of California, Mexico. *Journal of Volcanology and Geothermal Research*, *93*(1–2), 31–52.
Negrete-Aranda, R., & Canon-Tapia, E. (2008). Post-subduction volcanism in the Baja California Peninsula, Mexico: The effects of tectonic reconfiguration in volcanic systems. *Lithos*, *102*(1-2), 392–414. https://doi.org/10.1016/J.Lithos.2007.08.013
Negrete-Aranda, R., Canon-Tapia, E., Brandle, J. L., Ortega-Rivera, M. A., Lee, J. K. W., Spelz, R. M., & Hinojosa-Corona, A. (2010). Regional orientation of tectonic stress and the stress expressed by post-subduction high-magnesium volcanism in northern Baja California, Mexico: Tectonics and volcanism of San Borja volcanic field. *Journal of Volcanology and Geothermal Research, 192*(1–2), 97–115. doi: Doi https://doi.org/10.1016/J.Jvolgeores.2010.02.014.
Pallares, C., Maury, R. C., Bellon, H., Royer, J. Y., Calmus, T., Aguillón-Robles, A., et al. (2007). Slab-tearing following ridge-trench collision: Evidence from Miocene volcanism in Baja California, Mexico. *Journal of Volcanology and Geothermal Research*, *161*(1–2), 95–117. https://doi.org/10.1016/j.jvolgeores.2006.11.002

Reid, M. R., Bouchet, R. A., Blichert-Toft, J., Levander, A., Liu, K. J., Miller, M. S., & Ramos, F. C. (2012). Melting under the Colorado Plateau, USA. *Geology*, *40*(5), 387–390. https://doi.org/10.1130/G32619.1

Robinson, P. T., Elders, W. A., & Muffler, L. J. P. (1976). Quaternary volcanism in Salton Sea Geothermal Field, Imperial-Valley, California. *Geological Society of America Bulletin*, *87*(3), 347–360. https://doi.org/10.1130/0016-7606(1976)87<347:Qvitss>2.0.Co;2

Rukhlov, A. S., Blinova, A. I., & Pawlowicz, J. G. (2013). Geochemistry, mineralogy and petrology of the Eocene potassic magmatism from the Milk River area, southern Alberta, and Sweet Grass Hills, northern Montana. *Chemical Geology*, *353*, 280–302. https://doi.org/10.1016/j.chemgeo.2012.10.024

Saunders, A., Rogers, G., Marriner, G., Terrell, D., & Verma, S. (1987). Geochemistry of Cenezoic volcanic rocks, Baja California, Mexico: Implications for the petrogenesis of post-subduction magmas. *Journal of Volcanology and Geothermal Research*, *32*(1–3), 223–245.

Schmitt, A. K., Martin, A., Weber, B., Stockli, D. F., Zou, H. B., & Shen, C. C. (2013). Oceanic magmatism in sedimentary basins of the northern Gulf of California rift. *Geological Society of America Bulletin*, *125*(11–12), 1833–1850. https://doi.org/10.1130/B30787.1

Singer, K. I., & Fodor, F. V. (2013). Petrology of the Stewart Mountain basalt field in central Arizona, U.S.A.: A lithospheric source with small-scale trace element and isotopic heterogeneities. *Rocky Mountain Geology*, *48*, 185–210.

Turrin, B. D., Gutmann, J. T., & Swisher, C. C. (2008). A 13 ± 3 ka age determination of a tholeiite, Pinacate volcanic field, Mexico, and improved methods for Ar-40/Ar-39 dating of young basaltic rocks. *Journal of Volcanology and Geothermal Research*, *177*(4), 848–856. https://doi.org/10.1016/j.jvolgeores.2008.01.049

Vidal Solano, J. R., Lapierre, H., Stock, J. M., Demant, A., Paz Moreno, F. A., Bosch, D., et al. (2008). Isotope geochemistry and petrogenesis of peralkaline Middle Miocene ignimbrites from Central Sonora: Relationship with continental break-up and the birth of the Gulf of California. *Bulletin de la Societe Geologique de France*, *179*, 453–464.

Vidal-Solano, J. R., Demant, A., Moreno, F. A. P., Lapierre, H., Ortega-Rivera, M. A., & Lee, J. K. W. (2008). Insights into the tectono-magmatic evolution of NW Mexico: Geochronology and geochemistry of the Miocene volcanic rocks from the Pinacate area, Sonora. *Geological Society of America Bulletin*, *120*(5–6), 691–708. https://doi.org/10.1130/B26053.1

Wegert, D., Parker, D., & Ren, M. (2013). The Nathrop Domes, Colorado: Geochemistry and petrogenesis of a topaz rhyolite. *Rocky Mountain Geology*, *48*, 1–14.

Wolff, J. A., Ellis, B. S., Ramos, F. C., Starkel, W. A., Boroughs, S., Olin, P. H., & Bachmann, O. (2015). Remelting of cumulates as a process for producing chemical zoning in silicic tuffs: A comparision of cool, wet and hot, dry rhyolitic magma systems. *Lithos*, *236-237*, 275–286.